

Electronic Supplementary Information for:

**EXAFS Investigation of Temperature-Dependent Structure in Cobalt-59
Molecular NMR Thermometers**

Tyler M. Ozvat,^a George E. Sterbinsky,^b Anthony J. Campanella,^a Anthony K. Rappé,^a and Joseph M. Zadrozny^a

^a Department of Chemistry, Colorado State University, Fort Collins, Colorado 80523

^b X-ray Science Division, Argonne National Laboratory, Argonne, Illinois 60439

Table of Contents

Experimental Details	S4
XAS Measurement Details	S6
Structural Optimizations and SHAPE Analysis	S7
Figure S1 Series of Studied Co ³⁺ Complexes	S9
Table S1 Summary of Variable-Temperature EXAFS Measurements of r_1	S9
Table S2 Summary of Variable-Temperature EXAFS Fit Parameters of r_1 for 1-5	S10
Table S3 Figures of Merit for VT EXAFS Fits	S10
Figure S2 5 at 13 °C, R and k -space Fitted EXAFS Data	S11
Table S4 5 at 13 °C, EXAFS Fit Parameters	S11
Figure S3 5 at 35 °C, R and k -space Fitted EXAFS Data	S12
Table S5 5 at 35 °C, EXAFS Fit Parameters	S12
Figure S4 5 at 57 °C, R and k -space Fitted EXAFS Data	S13
Table S6 5 at 57 °C, EXAFS Fit Parameters	S13
Figure S5 4 at 13 °C, R and k -space Fitted EXAFS Data	S14
Table S7 4 at 13 °C, EXAFS Fit Parameters	S14
Figure S6 4 at 35 °C, R and k -space Fitted EXAFS Data	S15
Table S8 4 at 35 °C, EXAFS Fit Parameters	S15
Figure S7 4 at 57 °C, R and k -space Fitted EXAFS Data	S16
Table S9 4 at 57 °C, EXAFS Fit Parameters	S16
Figure S8 3 at 13 °C, R and k -space Fitted EXAFS Data	S17
Table S10 3 at 13 °C, EXAFS Fit Parameters	S17
Figure S9 3 at 35 °C, R and k -space Fitted EXAFS Data	S18
Table S11 3 at 35 °C, EXAFS Fit Parameters	S18
Figure S10 3 at 57 °C, R and k -space Fitted EXAFS Data	S19
Table S12 3 at 57 °C, EXAFS Fit Parameters	S19
Figure S11 2 at 13 °C, R and k -space Fitted EXAFS Data	S20
Table S13 2 at 13 °C, EXAFS Fit Parameters	S20
Figure S12 2 at 35 °C, R and k -space Fitted EXAFS Data	S21
Table S14 2 at 35 °C, EXAFS Fit Parameters	S21
Figure S13 2 at 57 °C, R and k -space Fitted EXAFS Data	S22
Table S15 2 at 57 °C, EXAFS Fit Parameters	S22
Figure S14 1 at 13 °C, R and k -space Fitted EXAFS Data	S23
Table S16 1 at 13 °C, EXAFS Fit Parameters	S23
Figure S15 1 at 35 °C, R and k -space Fitted EXAFS Data	S24
Table S17 1 at 35 °C, EXAFS Fit Parameters	S24
Figure S16 1 at 57 °C, R and k -space Fitted EXAFS Data	S25
Table S18 1 at 57 °C, EXAFS Fit Parameters	S25
Table S19 Change in N–Co–N Bite Angle of Optimized Structures in 2	S26
Table S20 Change in N–Co–N Bite Angle of Optimized Structures in 3	S26
Table S21 Change in N–Co–N Bite Angle of Optimized Structures in 5	S26
Table S22 SHAPE Analysis of O_h Symmetry in Optimized Structures 1-5	S27
Table S23 SHAPE Analysis of D_{3h} Symmetry in Optimized Structures 1-5	S27
Figure S17 Detailed depiction of bond angle changes in 4 .	S28
Table S24 Computed Structure [Co(diNOsar)] ³⁺ at 13 °C	S29
Table S25 Computed Structure [Co(diNOsar)] ³⁺ at 57 °C	S30
Table S26 Computed Structure [Co(tame) ₂] ³⁺ at 13 °C	S31

Table S27	Computed Structure $[\text{Co}(\text{tame})_2]^{3+}$ at 57 °C	S33
Table S28	Computed Structure $[\text{Co}(\text{tn})_3]^{3+}$ at 13 °C	S34
Table S29	Computed Structure $[\text{Co}(\text{tn})_3]^{3+}$ at 57 °C	S35
Table S30	Computed Structure $[\text{Co}(\text{en})_3]^{3+}$ at 13 °C	S36
Table S31	Computed Structure $[\text{Co}(\text{en})_3]^{3+}$ at 57 °C	S37
Table S32	Computed Structure $[\text{Co}(\text{NH}_3)_6]^{3+}$ at 13 °C	S38
Table S33	Computed Structure $[\text{Co}(\text{NH}_3)_6]^{3+}$ at 57 °C	S39
References		S40

Experimental Section

General Considerations. Studied compounds in this manuscript were either purchased from commercial chemical vendors or synthesized according previously reported literature preparations. Potassium hexacyanocobaltate(III) ($K_3[Co(CN)_6]$) and hexamminecobalt(III) chloride ($[Co(NH_3)_6]Cl_3$, **1**) were purchased from commercial vendors and used as received. The remaining compounds of study **2 – 5** were synthesized following literature preparations, and the exact procedures used are replicated below for full disclosure. 1H -NMR, ^{13}C -NMR, and ^{59}Co -NMR spectra were collected on a 400 MHz Bruker spectrometer. UV-Vis spectra were collected on an Agilent 8453 Spectrophotometer, and IR spectra were collected using a diamond ATR on a Bruker Tensor II FTIR.

[Co(en)₃]Cl₃·3H₂O (2). Synthesis of tris(1,2-diaminoethane)cobalt(III) chloride was done following previously reported literature preparations.¹ Cobalt(II) chloride hexahydrate (20.0 g, 154.05 mmol) was first dissolved in water (60 mL), while 12.1 M HCl (7.0 mL) was added dropwise to an ice-cooled solution of 1,2-diaminoethane (15.5 mL, 231.06 mmol) in water (40 mL) in a separate flask. To this partially neutralized mixture, the pre-made solution of cobalt(II) chloride hexahydrate was added with stirring, followed by 30% hydrogen peroxide (16.7 mL). After allowing the reaction flask to vent, the reaction mixture was gently boiled down to approximately 90 mL volume. While still hot, but not boiling, an equal volume of 12.1 M HCl was added portion-wise followed by ethanol (180 mL). The mixture was cooled to room temperature before cooling in an ice-bath. The precipitate was filtered and washed with ethanol (2 x 40 mL) and ethyl ether (2 x 40 mL) to provide an orange-colored crystalline salt (15.85 g, 30%). ^{59}Co NMR (500 MHz, H₂O): δ (ppm) 7145. IR (cm⁻¹, ATR): 438 (vs), 471 (m), 580 (w/s), 706 (s/vw), 780 (s), 898 (s/vw), 1057 (s), 1124 (s/w), 1156 (s), 1254 (s/vw), 1280 (s/vw), 1326 (s/w), 1364 (s/w), 1439 (m), 1463 (s), 1561 (s), 1583 (m), 3096 (s), 3204 (m), 3484 (m). UV-Vis (H₂O): λ_{max} (nm) (ϵ_M (M⁻¹cm⁻¹)): 338 (81) and 465 (83). Anal. Calcd. (Found) for C₆H₂₄Cl₃CoN₆·3H₂O: 18.03 (17.59) %C, 7.57 (7.55) %H, and 21.02 (20.95) %N.

[Co(tn)₃]Cl₃·5H₂O (3). Synthesis of tris(1,3-diaminoethane)cobalt(III) chloride was done following previously reported literature preparations.² A solution of 1,3-diaminopropane (30.9 mL, 369.7 mmol) in water (10 mL) was partially neutralized with the dropwise addition of 12.1 M HCl (7.6 mL, 92.4 mmol). Cobalt(II) chloride hexahydrate (12.0 g, 92.4 mmol) in water (40 mL) was then carefully added to the diamine solution with stirring. Activated charcoal (1.0 g) was added, then air was bubbled through the stirring solution for 20 h before filtering off the charcoal with multiple rinses of water. The collected filtrate was concentrated to 20 mL before transferring to ethanol (200 mL) and cooled on an ice bath. The resulting precipitate was filtered and sequentially washed with ethanol and diethyl ether to yield a dark brown-pink residue. The product was recrystallized from hot water before additional ethanol (100 mL) was added and cooled on an ice bath. The resulting precipitate was filtered and washed with diethyl ether to yield a yellow-pink precipitate. Yield: 9.96 g, 28%. 1H NMR (400 MHz, D₂O): δ (ppm) 2.59 (d, 12H), 1.87 (t, 6H). ^{59}Co NMR (500 MHz, H₂O): δ (ppm) 8340. IR (cm⁻¹, diamond ATR): 420 (s), 448 (w/s), 488 (w/s), 515 (w/s), 520 (s), 690 (m/w), 720 (s/vw), 733 (s/vw), 886 (s/w), 931 (s), 1039 (vs),

1088 (s/vw), 1138 (m/vw), 1185 (s), 1208 (s/w), 1234 (s), 1274 (m/w), 1310 (s/vw), 1362 (m/w), 1413 (m/w), 1456 (s/vw), 1478 (w/s), 1571 (m), 2888 (w/s), 2962 (m), 3090 (s), 3151 (m), 3392 (m/w). UV-Vis (H₂O, Fig. 2): λ_{max} (nm) (ϵ_{M} (M⁻¹cm⁻¹)): 350 (76) and 485 (74). Anal. Calcd. (Found) for C₉H₃₀Cl₃CoN₆·3.5H₂O: 23.98 (24.11) %C, 8.27 (8.06) %H, and 18.64 (18.59) %N.

[Co(tame)₂]Cl₃·1.5H₂O (4). Synthesis of bis(1,1,1-tris(aminomethyl)ethane)cobalt(III) chloride³ and the 1,1,1-tris(aminomethyl)ethane trihydrochloride (tame·3HCl) starting material were done following previously reported literature preparations.⁴ Firstly, tame·3HCl (0.3070 g, 1.355 mmol) was dissolved in 5 mL of water and mixed with silver(I) oxide (0.6240 g, 6.14 mmol). The solution vessel was wrapped in aluminum foil, shaken vigorously for 5 min, and stirred for 2 hr. The dark turbid mixture of partially neutralized tame was filtered twice with water through a pipet plugged with cotton and celite to remove excess silver(I) oxide and silver(I) chloride precipitate. To the filtrate was added cobalt(II) chloride hexahydrate (0.1131 g, 0.475 mmol), resulting in a rapid dark, opaque black-brown color transition. After allowing the mixture to stir for 1 min, 1 M HCl (0.4 mL) and finely crushed activated charcoal (0.014 g) were added and stirred vigorously while bubbling air through the solution for 1 h. Within the first few minutes, the solution was observed to have a dark orange-brown tinge and allowed to stir overnight for 16 h without aeration. The mixture was concentrated to a minimal volume under mild heat and flowing air before allowing the solution to return to room temperature. The concentrate was further cooled in an ice-bath yielding solid orange crystals and subsequently washed with multiple small portions of cold acetone and ethanol (1:1). The crystalline product was afforded as orange hexagonal platelets (0.1046 g, 55%). ⁵⁹Co NMR (500 MHz, H₂O): δ (ppm) 7409. IR (cm⁻¹, ATR): 424 (vs), 571 (vw/s), 745 (m/vw), 815 (m/vw), 888 (m/vw), 908 (s/w), 1009 (s), 1068 (s/vw), 1128 (s/vw), 1153 (s/w), 1227 (m), 1310 (m/vw), 1349 (s/vw), 1373 (m/vw), 1401 (s/vw), 1460 (s/w), 1500 (m/vw), 1545 (m/vw), 1594 (m), 1600 (m), 2884 (s/w), 2947 (m), 3027 (s), 3150 (m), 3499 (m). UV-Vis (H₂O, Fig. 2): λ_{max} (nm) (ϵ_{M} (M⁻¹cm⁻¹)): 338 (67) and 468 (78). Anal. Calcd. (Found) for C₁₀H₃₀Cl₃CoN₆·1.5H₂O: 28.15 (28.31) %C, 7.79 (7.45) %H, and 19.64 (19.62) %N.

[Co(diNOsar)]Cl₃·2H₂O (5). Synthesis of (1,8-dinitro-3,6,10,13,16,19-hexaazabicyclo[6.6.6]icosane)cobalt(III) chloride, also known as dinitrosarcophagine, was done following previously reported literature preparations.⁵ To a solution of [Co(en)₃]Cl₃ (8.66 g, 25 mmol) dissolved into water (50 mL), nitromethane (5.37 mL, 100 mmol) and 37% formaldehyde (26.2 mL, 950 mmol) was added. Subsequently, a solution of 4 M NaOH (17.18 mL, 68.75 mmol) was added dropwise resulting in a deep violet-brown mixture. The mixture was allowed to stir for 2 h before the addition of 12.1 M HCl (8.26 mL, 100 mmol) which became a transparent orange solution. The product was precipitated by cooling the mixture in an ice-bath and collected by filtration with multiple washings of cold methanol. The chloride salt product was collected as an orange powder (4.300 g, 31.8%). ⁵⁹Co NMR (500 MHz, H₂O): δ (ppm) 6894. IR (cm⁻¹, diamond ATR): 438 (s/w), 467 (s), 503 (m), 597 (vs/w), 621 (s/vw), 787 (vs/w), 812 (vs), 840 (s/w), 873 (s/w), 952 (s/w), 974 (m/vw), 1019 (s/w), 1060 (m), 1077 (m), 1131 (m/vw), 1171 (s/vw), 1198 (s/vw), 1236 (s/vw), 1271 (s/vw), 1342 (s), 1382 (s/vw), 1429 (s/vw), 1453 (m), 1555 (vs), 1602 (m/w), 1655 (m/vw), 2375 (m/vw), 2947 (m), 3004 (m/w), 3032 (m), 3409 (m/w), 3466 (m/w). UV-Vis (H₂O, Fig. 2): λ_{max}

(nm) (ϵ_M ($M^{-1}cm^{-1}$)): 342 (204) and 475 (161). Anal. Calcd. (Found) for $C_{14}H_{30}Cl_3CoN_8O_4 \cdot 2H_2O$: 29.21 (29.32) %C, 5.95 (5.70) %H, and 19.46 (19.36) %N.

XAS Measurement Details

Sample Preparation. XAFS measurements made on compounds **1** – **5** were collected from samples of each compound which were prepared as described below. Compound **1** was purchased from a chemical vendor and compounds **2** – **5** were synthesized as reported above. All hydrate-forming compounds were thoroughly dried of water in a high-vac oven over 24 hrs. Sample amounts of each compound were then accurately weighed out and prepared as 15 mM solutions in Millipore purified deionized water. Fluorescence mode XAFS measurements require dilute atomic concentrations of the absorbing atom in order to minimize self-absorption artefacts. Seeking an atomic concentration below 5% for our studies, a 15 mM concentration was chosen for these experiments as calculated for an atomic concentration of 2.5 – 2.7 % for the absorbing cobalt atom.

VT EXAFS Fluorescence Measurements. Variable-temperature X-ray absorption fine structure (XAFS) measurements were conducted at Beamline 9-BM of the Advanced Photon Source (APS) at Argonne National Laboratory. 4 mL aliquots of the 15 mM solutions of **1-5** were transferred into a polyetheretherketone (PEEK) cuvette and capped with an insertable thermocouple. Energy calibration was achieved by alignment to the Co *K*-absorption edge of 7708.78 eV using a cobalt foil standard. The beryllium windowed four-element silicon-drift fluorescence detector was positioned at the center of the PEEK cuvette. Subsequent Co *K*-edge X-ray absorption measurements were recorded from fluorescence detection of the Co- $K\alpha$ emission. Individual scans occurred in steps of 0.05 \AA^{-1} with 0.5 s integration times over *k*-range 0 – 15 \AA^{-1} . The integration time was progressively increased as energy increased through the EXAFS region of the scan. Each experiment consisted of 8 – 12 collected scans per sample measurement at each temperature. Temperature-specific XAFS measurements were made at 13, 35, and 57 °C. Thermal regulation of the contained sample occurred by fitting the cuvette to a water-jacketed cuvette holder equipped with a temperature-controllable water recirculator. Thermal equilibration of samples were monitored by thermocouple readouts of the solution before performing XAFS experiments. Sample temperatures were closely monitored throughout the experiment and did not deviate more than $\pm 1.0 \text{ }^\circ\text{C}$.

EXAFS Analysis. Extended X-ray absorption fine structure (EXAFS) spectra were acquired from the variable-temperature XAS data in which the EXAFS regions were analyzed. Scans for each compound were averaged before rebinning the k^2 -weighted EXAFS data. All data reduction and fits were made using the Demeter: XAS Data Processing and Analysis software using IFEFFIT.⁶ In the completed investigation of dynamic structural change between differing ligand compositions, the Fourier transform (FT) data of all solution-phase EXAFS spectra were fit against their respective crystal structures as each has been previously reported.⁷⁻¹¹ Calculated scattering paths from these experimental solid-stated models were then used to construct fits elucidating the relative changes in bond lengths and degrees of atomic displacements between each solution-

phase compound. The calculated scattering paths from the crystal-structure models were used to construct a complete fit for all spectra over k -range of 2-12 \AA^{-1} (Figs. S2-S16). The magnitudes and real parts of the Fourier transforms of $k^2\chi(k)$ along with the resulting fits are shown in Figs. S2-S16. All R -space fits were taken with k , k^2 , k^3 -weighting from which S_0^2 , E_0 , ΔR , and σ^2 parameters were evaluated from the fitting software Artemis.⁶ Atomic distances R were determined from ΔR of the fit, where $\Delta R = R - R_{\text{eff}}$ and R_{eff} is the atomic distance for a specified set of atoms in the reference model structure, and was determined with the ATOMS function in Artemis,¹² using the provided crystal structure data.⁷⁻¹¹ In the fitting process, ΔR was evaluated using a proportionality coefficient α (a solvable parameter) where $\Delta R = \alpha \times R_{\text{eff}}$. Ultimately, absolute atomic distances were evaluated from $R = R_{\text{eff}} (\alpha + 1)$.

The chosen experimental models provide acceptable fits across all solution-phase compounds of the primary and secondary coordination shells within 1-3 \AA of the FT data presented in R -space as radial structure functions, not radial distributions. All fits were made with single scattering paths to known atomic ligand shells and were complemented with smaller-angle double scattering type pathways. The inclusion of these secondary scattering paths inherently increases the necessary fitting range and are greater for larger molecules e.g., **4** and **5**. As a result, **1** was only fit only to single scattering paths (i.e., Co–N) over an R -range of 1.1-2 \AA without double scattering pathways. Owing to solvent effects, challenges in fitting of **1** beyond the first coordination shell were expected and are reflected in the fit parameters.¹³⁻¹⁶ For all complexes, we assumed that all Co–N bond distances were equivalent, owing to the homoleptic nature of the complexes and the lack of any expected Jahn-Teller activity for the Co(III) ion.

Uncertainty in the values of Co–N bond distances r_1 (Table S2) were determined from the error in the proportionality coefficient α yielded from the fits. In Artemis, the statistically determined uncertainty in the fit parameters are multiplied by $\sqrt{\chi_v^2}$ to account for systematic errors. These systematic errors result largely from imperfect background subtraction used to extract the EXAFS from the X-ray absorption and error and imperfect calculations of the photoelectron phase shifts and scattering amplitudes used to fit the data. Here, the same background subtraction procedure was used for all data sets, and fits of the three EXAFS temperature measurement (13, 35, and 57 $^\circ\text{C}$) were made in tandem to the same respective crystal structure model. Thus, these systematic errors will be the same for fits to a given compound at all temperatures, and they will cancel in a relative comparison. In this case, noise in the data and the stability in the energy axis E (eV) over the course of the experiments determine the accuracy of the relative bond-length measurements. In VT EXAFS studies, accuracies within $\pm 0.0001 \text{ \AA}$ have been observed.¹⁷⁻²⁰ Due to the inherent stability of the X-ray energy estimated to be within 0.05 eV, the accuracies of relative bond distance changes are within $\pm 0.0005 \text{ \AA}$ in the absence of noise and systematic errors.²¹ To account for noise in the data, we have divided the uncertainty in α calculated by Artemis by $\sqrt{\chi_v^2}$, and used that value for calculation of the uncertainty in ΔR . Based on the assumption that systematic errors are greatly reduced in a relative comparison of the bond lengths, we have added the estimated uncertainties due to energy stability and noise to obtain the total uncertainty reported for relative differences in Co–N bond lengths for a given molecule.

Structural Optimizations and SHAPE Analysis. Structural optimizations of complexes **1-5** were made at the low (13 °C) and high temperature (57 °C) bond lengths elucidated from solution-phase EXAFS bond distance determination of r_1 . Optimizations of each structure were made with Gaussian 16 electronic structure package²² using the ω B97xd density functional²³ and 6-311+g* basis set.²⁴ The resulting atomic coordinates are given in Tables S24 to S33. Changes in the N–Co–N angles of bidentate ligands (the “bite” angles) of **2**, **3**, **4**, and **5** were determined from the optimized structures (Tables S19-S21, Fig. S17). The change in coordination geometries between the minimized structures at 13 and 57 °C were then analyzed via SHAPE²⁵⁻²⁷ to determine relative changes between idealized octahedral and trigonal prismatic symmetries (Tables S22-S23).

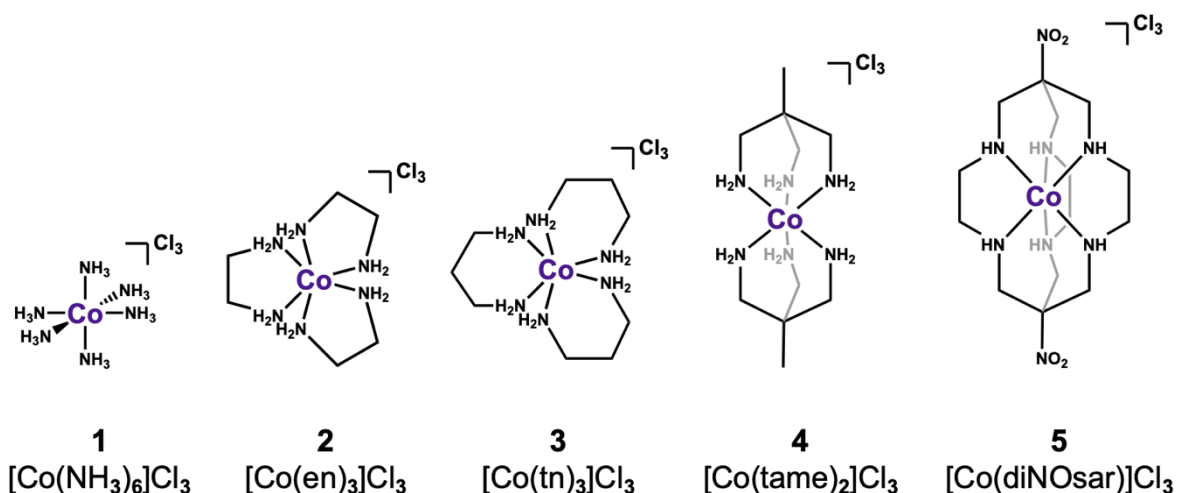


Figure S1 | Bond-line chemical structure representations of the five Co³⁺ studied complexes in this manuscript. All complexes are studied as 15 mM solutions in water as chloride salts. Hydrogens bound to carbons are omitted for clarity

Table S1 | Variable-temperature EXAFS measurements of complexes **1** – **5** of the Co–N₆ bond lengths from single scattering distances of the primary coordination sphere. Measurements were made over ~50 °C temperature window between 13, 35, and 57 °C. Values of r_1 (Å) were elucidated from fits of the EXAFS data (pages S9-S17). Determination of uncertainties in r_1 are detailed in above. Values of r_1 are the same as reported in Table S2. Reported Δr_1 values are between the 13 and 57 °C data.

		Co–N₆ Radial Distance, r_1 (Å)			
Structure	13 °C	35 °C	57 °C	Δr_1	
1 [Co(NH ₃) ₆]Cl ₃	1.9588(5)	1.9742(6)	1.9836(5)	0.0248(6)	
2 [Co(en) ₃]Cl ₃	1.9694(5)	1.9706(5)	1.9714(5)	0.0020(5)	
3 [Co(tn) ₃]Cl ₃	1.9825(5)	1.9881(5)	1.9910(5)	0.0085(5)	
4 [Co(tame) ₂]Cl ₃	1.9700(5)	1.9698(5)	1.9707(5)	0.0007(5)	
5 [Co(diNOsar)]Cl ₃	1.9701(5)	1.9751(6)	1.9776(6)	0.0075(6)	

Table S2 | Variable-temperature EXAFS fit parameters of **1-5** made specifically for the Co–N₆ distance of the first shell. All temperature-specific data for a given complex were fit collectively to their respective crystal structure models with a common amplitude reduction factor S_0^2 , and E_0 (eV). Values of r_1 are the same as reported in Table S1.^a

	Temp (°C)	S_0^2	E_0	α	σ^2 (Co–N ₆)	ΔR (Å)	R_{eff} (Å)	r_1 (Å)
1	13	0.475(55)	0.14(1.2)	-0.005(6)	-0.0006(14)	-0.00991	1.9687	1.9588(5)
	35	0.475(55)	0.14(1.2)	0.003(9)	-0.0012(23)	0.00545	1.9687	1.9742(6)
	57	0.475(55)	0.14(1.2)	0.008(6)	0.0076(61)	0.01488	1.9687	1.9836(5)
2	13	0.644(27)	3.30(39)	0.007(2)	0.0004(6)	0.01448	1.9549	1.9694(5)
	35	0.644(27)	3.30(39)	0.008(2)	0.0006(4)	0.01569	1.9549	1.9706(5)
	57	0.644(27)	3.30(39)	0.008(2)	0.0012(4)	0.01648	1.9549	1.9714(5)
3	13	0.761(31)	1.21(46)	-0.008(2)	0.0002(4)	-0.01665	1.9991	1.9825(5)
	35	0.761(31)	1.21(46)	-0.005(2)	0.0019(5)	-0.01097	1.9991	1.9881(5)
	57	0.761(31)	1.21(46)	-0.004(1)	0.0021(4)	-0.00813	1.9991	1.9910(5)
4	13	0.895(27)	2.17(34)	-0.001(1)	0.0012(3)	-0.00259	1.9726	1.9700(5)
	35	0.895(27)	2.17(34)	-0.001(1)	0.0016(4)	-0.0028	1.9726	1.9698(5)
	57	0.895(27)	2.17(34)	-0.001(1)	0.0016(3)	-0.00195	1.9726	1.9707(5)
5	13	0.924(40)	1.17(44)	-0.006(2)	0.0013(5)	-0.01188	1.9820	1.9701(5)
	35	0.924(40)	1.17(44)	-0.004(1)	0.0026(4)	-0.00694	1.9820	1.9751(6)
	57	0.924(40)	1.17(44)	-0.002(2)	0.0024(5)	-0.00442	1.9820	1.9776(6)

^a Note that ΔR in this table and Δr_1 commonly used in the manuscript are distinct values. ΔR (Å) is determined by $\Delta R = r_1 - R_{\text{eff}}$, and Δr_1 (Å) is the difference in r_1 between 13 and 57 °C EXAFS measurements (plotted in Fig. 3 of manuscript).

Table S3 | Evaluation of fit parameters χ^2 , reduced- χ^2 , R-factor, number of independent points N_{ind} , and number of variables N_{var} , over the selected fit ranges for **1-5**. These parameters apply to all temperature-specific data for a compound as each set was made in the same fit.

	1	2	3	4	5
χ^2	630474.56	558155.64	473168.89	193677.43	193966.20
χ_v^2	70782.37	12412.08	9438.67	4109.35	4395.25
R-factor	0.038375	0.0241832	0.0189678	0.0126918	0.023611
N_{ind}	19.9	56.0	64.1	64.1	64.1
N_{var}	8	11	14	17	20

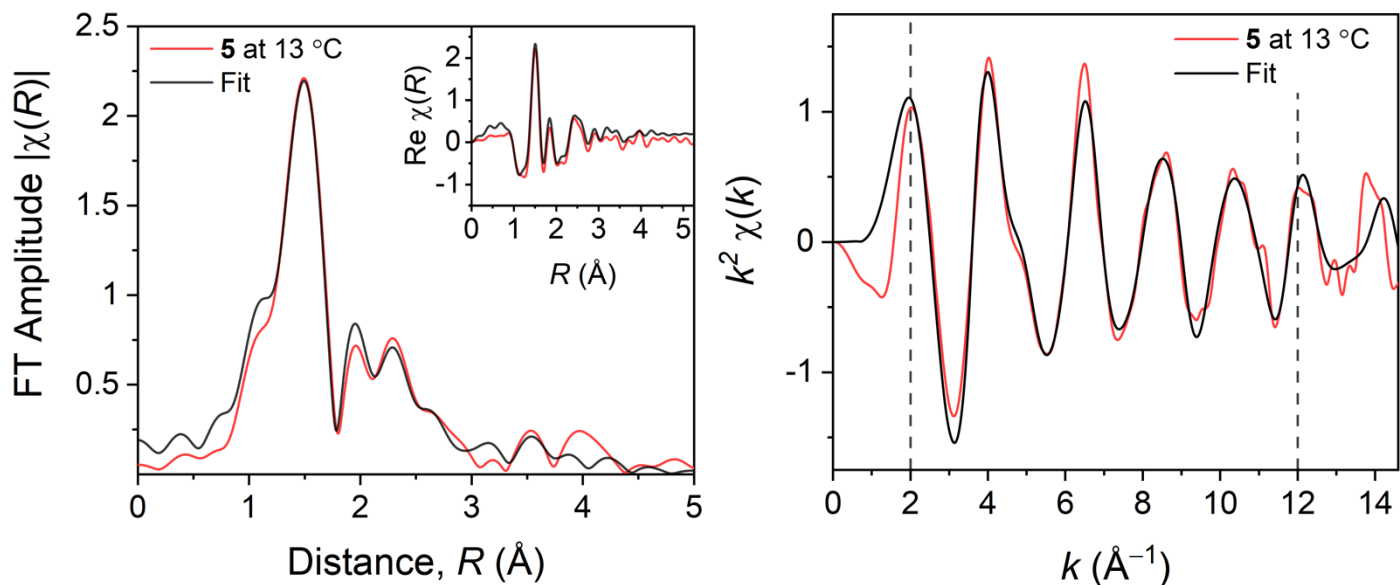


Figure S2 | Derived R -space (*left*) and k -space (*right*) plots of EXAFS fluorescence measured spectra for **5** at 13 °C at the Co K -edge (0 – 15 Å⁻¹ at $\Delta k = 0.05$ Å⁻¹). EXAFS data (*red*) against simulated fits (*black*) are made with k^2 -weighting over R -range of 1.1 – 4.5 Å and k -range of 2 – 12 Å⁻¹. **Inset:** Fit of real part of the FT EXAFS data. Fits were made according to reported crystal structure data.¹¹

Table S4 | EXAFS fit parameters of single scatter pathways for **5** at 13 °C.

Path	Atom Type	N	R_{eff} (Å)	ΔR (Å)	r (Å)	σ^2 (Å ²)
r_1	N	6	1.9820	-0.01188	1.97012	0.0013(5)
r_2	C	6	2.8153	-0.01688	2.79842	0.003(2)
r_3	C	6	2.9957	-0.01796	2.97774	0.004(4)
r_4	C	2	3.0221	-0.01812	3.00398	0.04(15)

Common fit parameters for this set include $S_0^2 = 0.92(4)$, $E_0 = 1.2(4)$ eV, and $\alpha = -0.006(2)$

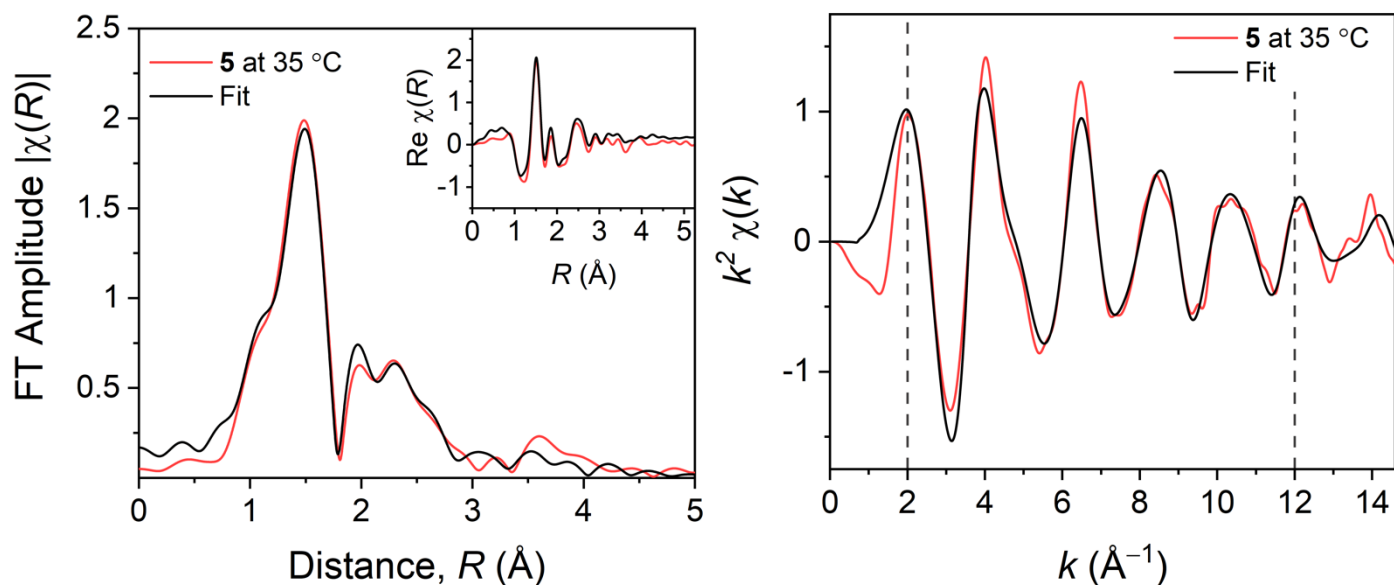


Figure S3 | Derived R -space (*left*) and k -space (*right*) plots of EXAFS fluorescence measured spectra for **5** at 35 °C at the Co K -edge (0 – 15 Å⁻¹ at $\Delta k = 0.05$ Å⁻¹). EXAFS data (*red*) against simulated fits (*black*) are made with k^2 -weighting over R -range of 1.1 – 4.5 Å and k -range of 2 – 12 Å⁻¹. **Inset:** Fit of real part of the FT EXAFS data. Fits were made according to reported crystal structure data.¹¹

Table S5 | EXAFS fit parameters of single scatter pathways for **5** at 35 °C.

Path	Atom Type	N	R_{eff} (Å)	ΔR (Å)	r (Å)	σ^2 (Å ²)
r_1	N	6	1.9820	-0.0069	1.97506	0.0026(4)
r_2	C	6	2.8153	-0.00986	2.80544	0.004(1)
r_3	C	6	2.9957	-0.01049	2.98521	0.007(3)
r_4	C	2	3.0221	-0.01059	3.01151	0.03(4)

Common fit parameters for this set include $S_0^2 = 0.92(4)$, $E_0 = 1.2(4)$ eV, and $\alpha = -0.004(1)$

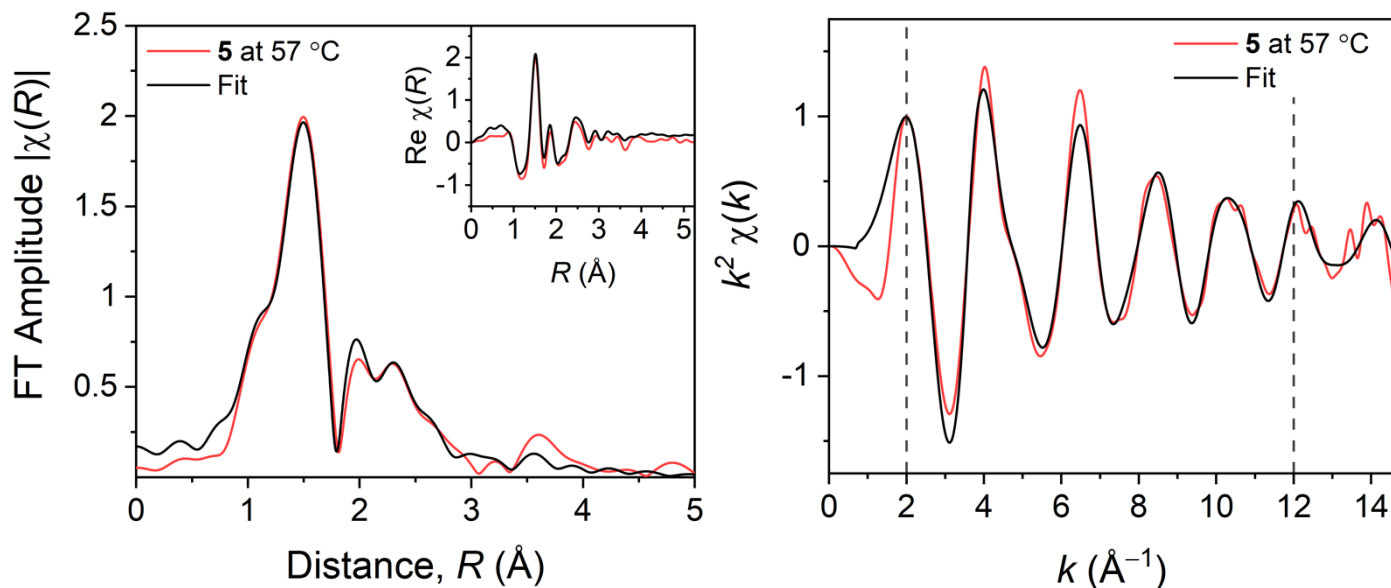


Figure S4 | Derived R -space (*left*) and k -space (*right*) plots of EXAFS fluorescence measured spectra for **5** at 57 °C at the Co K -edge (0 – 15 Å⁻¹ at $\Delta k = 0.05$ Å⁻¹). EXAFS data (*red*) against simulated fits (*black*) are made with k^2 -weighting over R -range of 1.1 – 4.5 Å and k -range of 2 – 12 Å⁻¹. **Inset:** Fit of real part of the FT EXAFS data. Fits were made according to reported crystal structure data.¹¹

Table S6 | EXAFS fit parameters of single scatter pathways for **5** at 57 °C.

Path	Atom Type	N	R_{eff} (Å)	ΔR (Å)	r (Å)	σ^2 (Å ²)
r_1	N	6	1.982	-0.00442	1.97758	0.0024(5)
r_2	C	6	2.8153	-0.00628	2.80902	0.005(2)
r_3	C	6	2.9957	-0.00669	2.98901	0.01(1)
r_4	C	2	3.0221	-0.00674	3.01536	0.02(6)

Common fit parameters for this set include $S_0^2 = 0.92(4)$, $E_0 = 1.2(4)$ eV, and $\alpha = -0.002(2)$

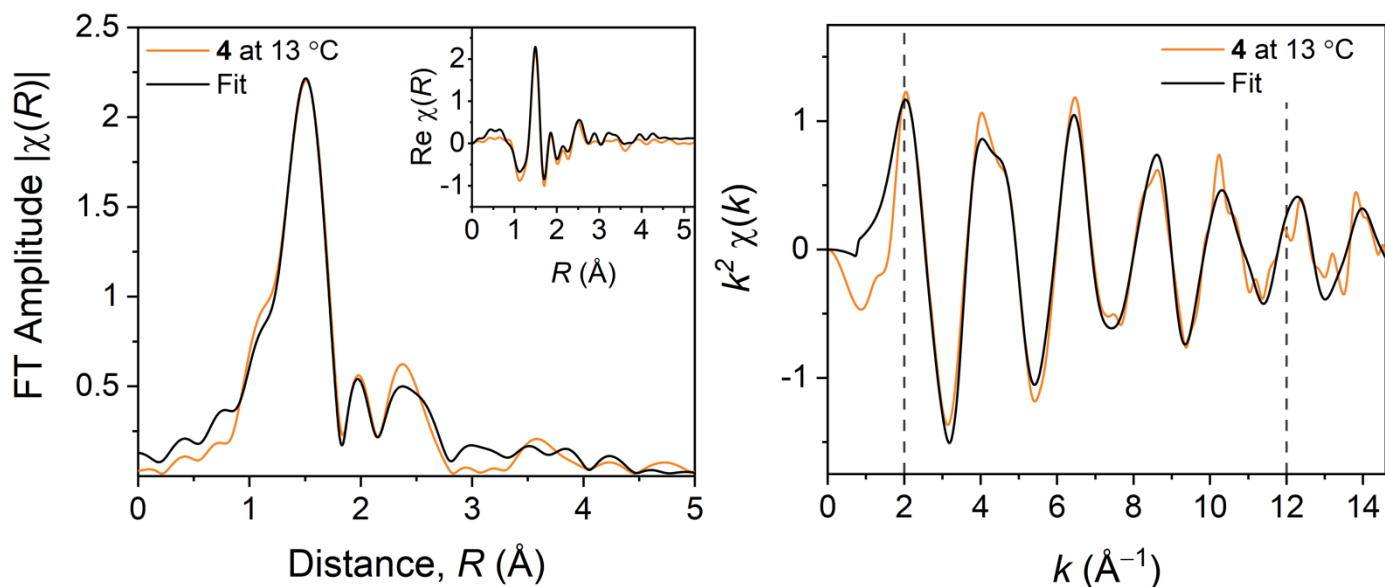


Figure S5 | Derived R -space (*left*) and k -space (*right*) plots of EXAFS fluorescence measured spectra for **4** at 13 °C at the Co K -edge (0 – 15 Å⁻¹ at $\Delta k = 0.05$ Å⁻¹). EXAFS data (*brown*) against simulated fits (*black*) are made with k^2 -weighting over R -range of 1.1 – 4.5 Å and k -range of 2 – 12 Å⁻¹. **Inset:** Fit of real part of the FT EXAFS data. Fits were made according to reported crystal structure data.¹⁰

Table S7 | EXAFS fit parameters of single scatter pathways for **4** at 13 °C.

Path	Atom Type	N	R_{eff} (Å)	ΔR (Å)	r (Å)	σ^2 (Å ²)
r_1	N	6	1.9726	-0.00259	1.97001	0.0012(3)
r_2	C	6	2.9727	-0.0039	2.9688	0.003(1)
r_3	C	2	3.0861	-0.00405	3.08205	0.03(3)
r_4	C	2	4.6287	-0.00608	4.62262	0.06(19)

Common fit parameters for this set include $S_0^2 = 0.80(3)$, $E_0 = 2.2(3)$ eV, and $\alpha = -0.001(1)$

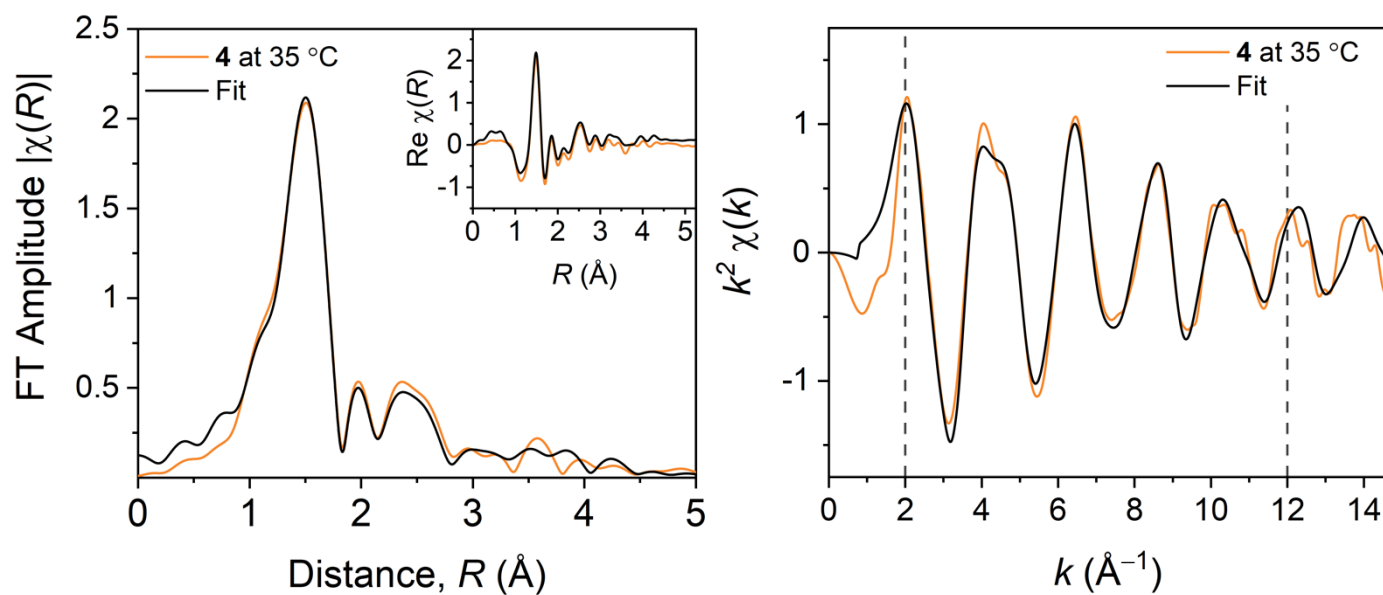


Figure S6 | Derived R -space (*left*) and k -space (*right*) plots of EXAFS fluorescence measured spectra for **4** at 35 °C at the Co K -edge (0 – 15 \AA^{-1} at $\Delta k = 0.05 \text{\AA}^{-1}$). EXAFS data (*brown*) against simulated fits (*black*) are made with k^2 -weighting over R -range of 1.1 – 4.5 \AA and k -range of 2 – 12 \AA^{-1} . **Inset:** Fit of real part of the FT EXAFS data. Fits were made according to reported crystal structure data.¹⁰

Table S8 | EXAFS fit parameters of single scatter pathways for **4** at 35 °C.

Path	Atom Type	N	R_{eff} (\AA)	ΔR (\AA)	r (\AA)	σ^2 (\AA^2)
r_1	N	6	1.9726	-0.0028	1.9698	0.0016(4)
r_2	C	6	2.9727	-0.00422	2.96848	0.003(1)
r_3	C	2	3.0861	-0.00438	3.08172	0.02(2)
r_4	C	2	4.6287	-0.00656	4.62214	0.01(4)

Common fit parameters for this set include $S_0^2 = 0.80(3)$, $E_0 = 2.2(3)$ eV, and $\alpha = -0.001(1)$

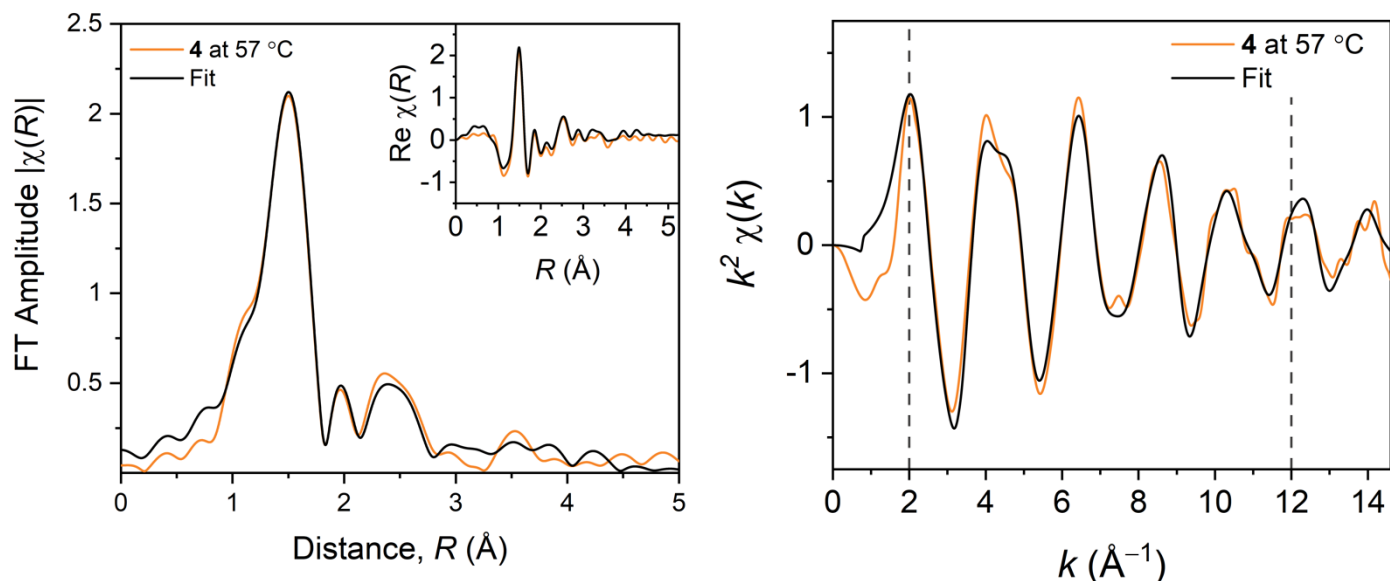


Figure S7 | Derived R -space (*left*) and k -space (*right*) plots of EXAFS fluorescence measured spectra for **4** at 57 °C at the Co K -edge (0 – 15 \AA^{-1} at $\Delta k = 0.05 \text{\AA}^{-1}$). EXAFS data (*brown*) against simulated fits (*black*) are made with k^2 -weighting over R -range of 1.1 – 4.5 \AA and k -range of 2 – 12 \AA^{-1} . **Inset:** Fit of real part of the FT EXAFS data. Fits were made according to reported crystal structure data.¹⁰

Table S9 | EXAFS fit parameters of single scatter pathways for **4** at 57 °C.

Path	Atom Type	N	R_{eff} (\AA)	ΔR (\AA)	r (\AA)	σ^2 (\AA^2)
r_1	N	6	1.9726	-0.00195	1.97065	0.0016(3)
r_2	C	6	2.9727	-0.00294	2.96976	0.003(1)
r_3	C	2	3.0861	-0.00306	3.08304	0.01(1)
r_4	C	2	4.6287	-0.00458	4.62412	0.002(9)

Common fit parameters for this set include $S_0^2 = 0.80(3)$, $E_0 = 2.2(3)$ eV, and $\alpha = -0.001(1)$

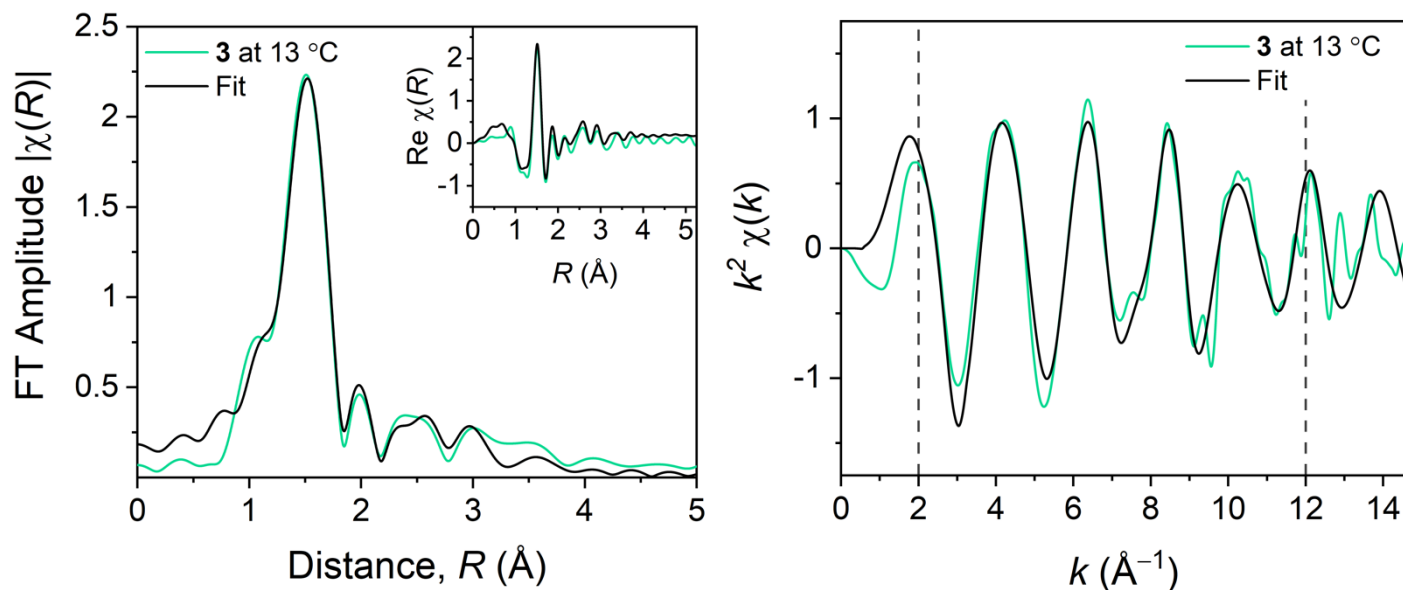


Figure S8 | Derived R -space (left) and k -space (right) plots of EXAFS fluorescence measured spectra for **3** at 13 °C at the Co K -edge (0 – 15 \AA^{-1} at $\Delta k = 0.05 \text{\AA}^{-1}$). EXAFS data (green) against simulated fits (black) are made with k^2 -weighting over R -range of 1.1 – 4.5 \AA and k -range of 2 – 12 \AA^{-1} . **Inset:** Fit of real part of the FT EXAFS data. Fits were made according to reported crystal structure data.⁹

Table S10 | EXAFS fit parameters of single scatter pathways for **3** at 13 °C.

Path	Atom Type	N	R_{eff} (\AA)	ΔR (\AA)	r (\AA)	σ^2 (\AA^2)
r_1	N	6	1.9991	-0.01665	1.98245	0.0002(4)
r_2	C	6	3.0372	-0.0253	3.0119	0.003(2)
r_3	C	3	3.4031	-0.02835	3.37475	0.05(7)

Common fit parameters for this set include $S_0^2 = 0.76(3)$, $E_0 = 1.2(5)$ eV, and $\alpha = -0.008(2)$

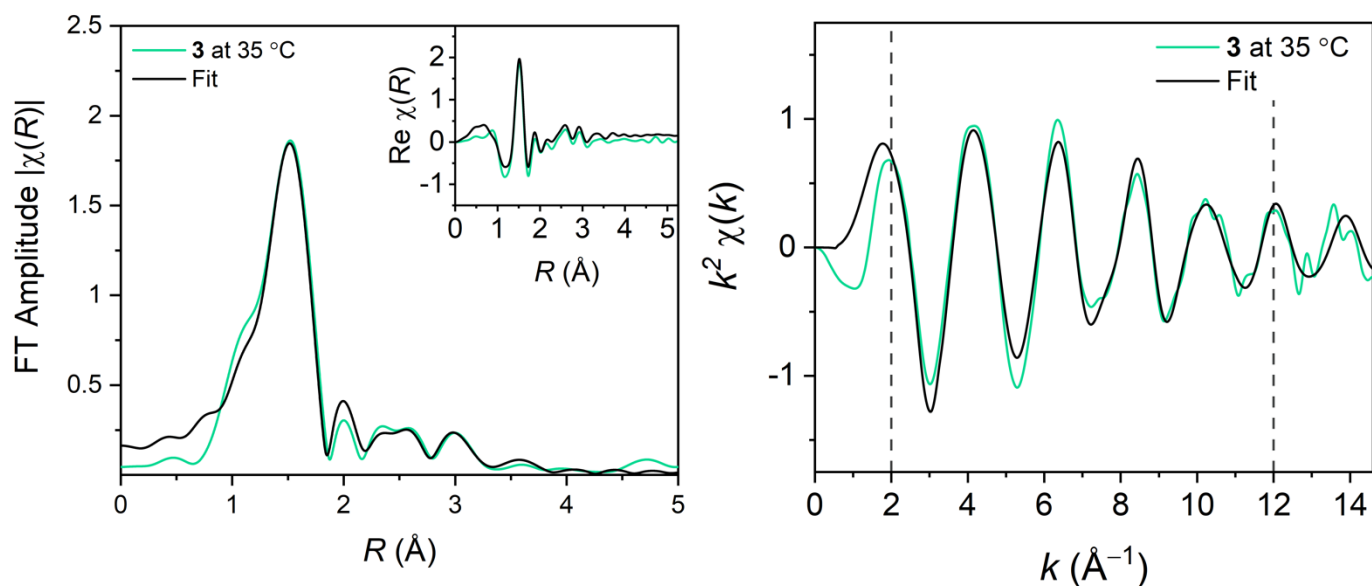


Figure S9 | Derived R -space (*left*) and k -space (*right*) plots of EXAFS fluorescence measured spectra for **3** at 35 °C at the Co K -edge (0 – 15 Å⁻¹ at $\Delta k = 0.05$ Å⁻¹). EXAFS data (*green*) against simulated fits (*black*) are made with k^2 -weighting over R -range of 1.1 – 4.5 Å and k -range of 2 – 12 Å⁻¹. **Inset:** Fit of real part of the FT EXAFS data. Fits were made according to reported crystal structure data.⁹

Table S11 | EXAFS fit parameters of single scatter pathways for **3** at 35 °C.

Path	Atom Type	N	R_{eff} (Å)	ΔR (Å)	r (Å)	σ^2 (Å ²)
r_1	N	6	1.9991	-0.01097	1.98813	0.0019(5)
r_2	C	6	3.0372	-0.01667	3.02053	0.006(3)
r_3	C	3	3.4031	-0.01867	3.38443	0.04(7)

Common fit parameters for this set include $S_0^2 = 0.76(3)$, $E_0 = 1.2(5)$ eV, and $\alpha = -0.005(2)$

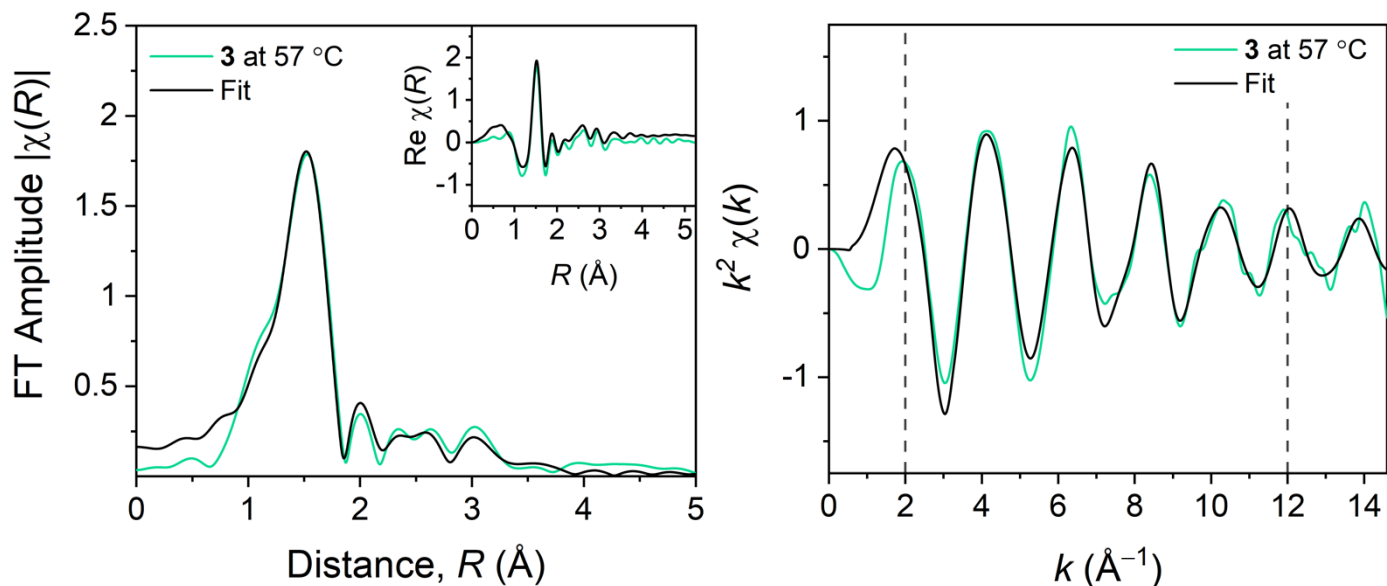


Figure S10 | Derived R -space (*left*) and k -space (*right*) plots of EXAFS fluorescence measured spectra for **3** at 57 °C at the Co K -edge (0 – 15 \AA^{-1} at $\Delta k = 0.05 \text{\AA}^{-1}$). EXAFS data (*green*) against simulated fits (*black*) are made with k^2 -weighting over R -range of 1.1 – 4.5 \AA and k -range of 2 – 12 \AA^{-1} . **Inset:** Fit of real part of the FT EXAFS data. Fits were made according to reported crystal structure data.⁹

Table S12 | EXAFS fit parameters of single scatter pathways for **3** at 57 °C.

Path	Atom Type	N	R_{eff} (\AA)	ΔR (\AA)	r (\AA)	σ^2 (\AA^2)
r_1	N	6	1.9991	-0.00813	1.99097	0.0021(4)
r_2	C	6	3.0372	-0.01235	3.02485	0.007(2)
r_3	C	3	3.4031	-0.01384	3.38926	0.05(6)

Common fit parameters for this set include $S_0^2 = 0.76(3)$, $E_0 = 1.2(5)$ eV, and $\alpha = -0.004(1)$

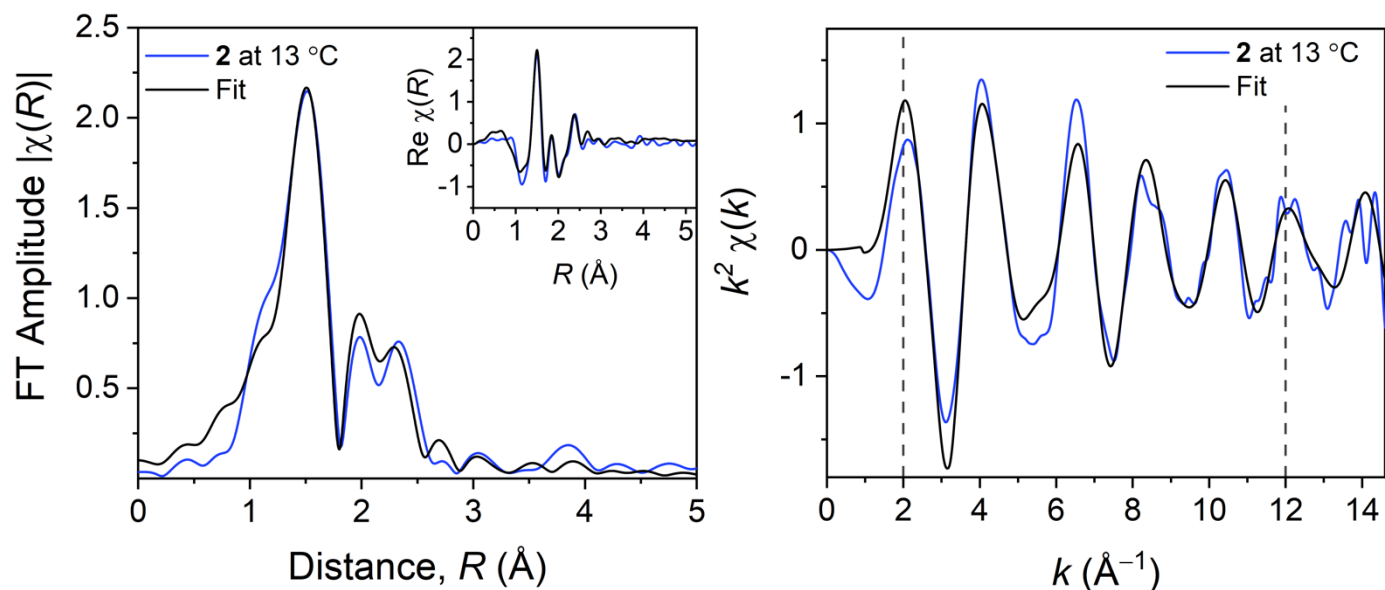


Figure S11 | Derived R -space (*left*) and k -space (*right*) plots of EXAFS fluorescence measured spectra for **2** at 13 °C at the Co K -edge (0 – 15 \AA^{-1} at $\Delta k = 0.05 \text{\AA}^{-1}$). EXAFS data (*blue*) against simulated fits (*black*) are made with k^2 -weighting over R -range of 1.1 – 4.2 \AA and k -range of 2 – 12 \AA^{-1} . **Inset:** Fit of real part of the FT EXAFS data. Fits were made according to reported crystal structure data.⁸

Table S13 | EXAFS fit parameters of single scatter pathways for **2** at 13 °C.

Path	Atom Type	N	R_{eff} (\AA)	ΔR (\AA)	r (\AA)	σ^2 (\AA^2)
r_1	N	6	1.9549	0.01448	1.96938	0.0004(6)
r_2	C	6	2.8207	0.02089	2.84159	0.002(1)

Common fit parameters for this set include $S_0^2 = 0.64(3)$, $E_0 = 3.3(4)$ eV, and $\alpha = 0.007(2)$

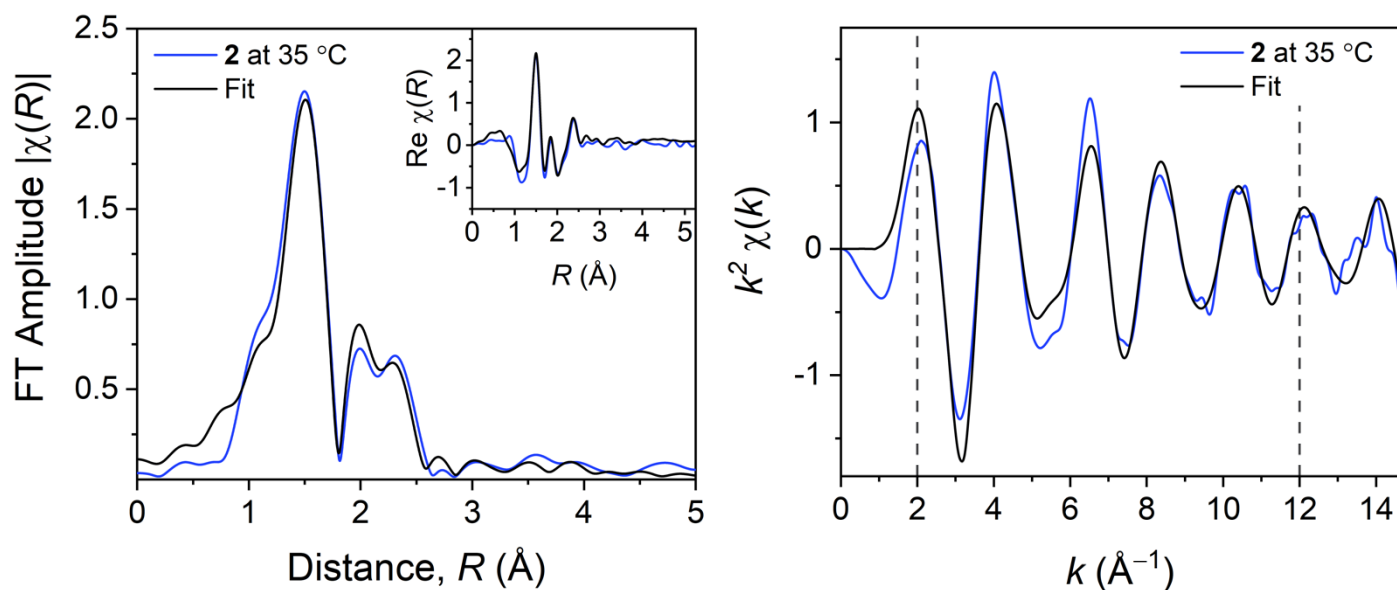


Figure S12 | Derived R -space (*left*) and k -space (*right*) plots of EXAFS fluorescence measured spectra for **2** at 35 °C at the Co K -edge ($0 - 15 \text{ \AA}^{-1}$ at $\Delta k = 0.05 \text{ \AA}^{-1}$). EXAFS data (*blue*) against simulated fits (*black*) are made with k^2 -weighting over R -range of $1.1 - 4.2 \text{ \AA}$ and k -range of $2 - 12 \text{ \AA}^{-1}$. **Inset:** Fit of real part of the FT EXAFS data. Fits were made according to reported crystal structure data.⁸

Table S14 | EXAFS fit parameters of single scatter pathways for **2** at 35 °C.

Path	Atom Type	N	$R_{\text{eff}} \text{ (\AA)}$	$\Delta R \text{ (\AA)}$	$r \text{ (\AA)}$	$\sigma^2 \text{ (\AA}^2\text{)}$
r_1	N	6	1.9549	0.01569	1.97059	0.0006(4)
r_2	C	6	2.8207	0.02264	2.84334	0.001(1)

Common fit parameters for this set include $S_0^2 = 0.64(3)$, $E_0 = 3.3(4) \text{ eV}$, and $\alpha = 0.008(2)$

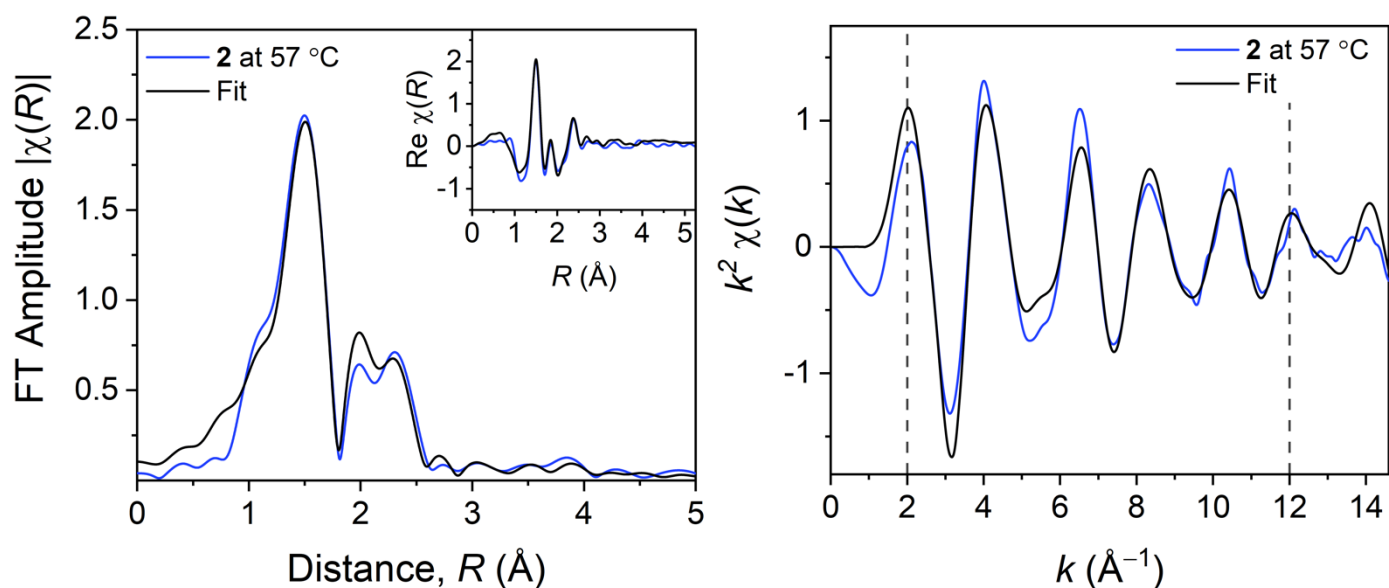


Figure S13 | Derived R -space (*left*) and k -space (*right*) plots of EXAFS fluorescence measured spectra for **2** at 57 °C at the Co K -edge ($0 - 15 \text{ \AA}^{-1}$ at $\Delta k = 0.05 \text{ \AA}^{-1}$). EXAFS data (*blue*) against simulated fits (*black*) are made with k^2 -weighting over R -range of $1.1 - 4.2 \text{ \AA}$ and k -range of $2 - 12 \text{ \AA}^{-1}$. **Inset:** Fit of real part of the FT EXAFS data. Fits were made according to reported crystal structure data.⁸

Table S15 | EXAFS fit parameters of single scatter pathways for **2** at 57 °C.

Path	Atom Type	N	$R_{\text{eff}} \text{ (\AA)}$	$\Delta R \text{ (\AA)}$	$r \text{ (\AA)}$	$\sigma^2 \text{ (\AA}^2\text{)}$
r_1	N	6	1.9549	0.01648	1.97138	0.0012(4)
r_2	C	6	2.8207	0.02378	2.84448	0.001(1)

Common fit parameters for this set include $S_0^2 = 0.64(3)$, $E_0 = 3.3(4) \text{ eV}$, and $\alpha = 0.008(2)$

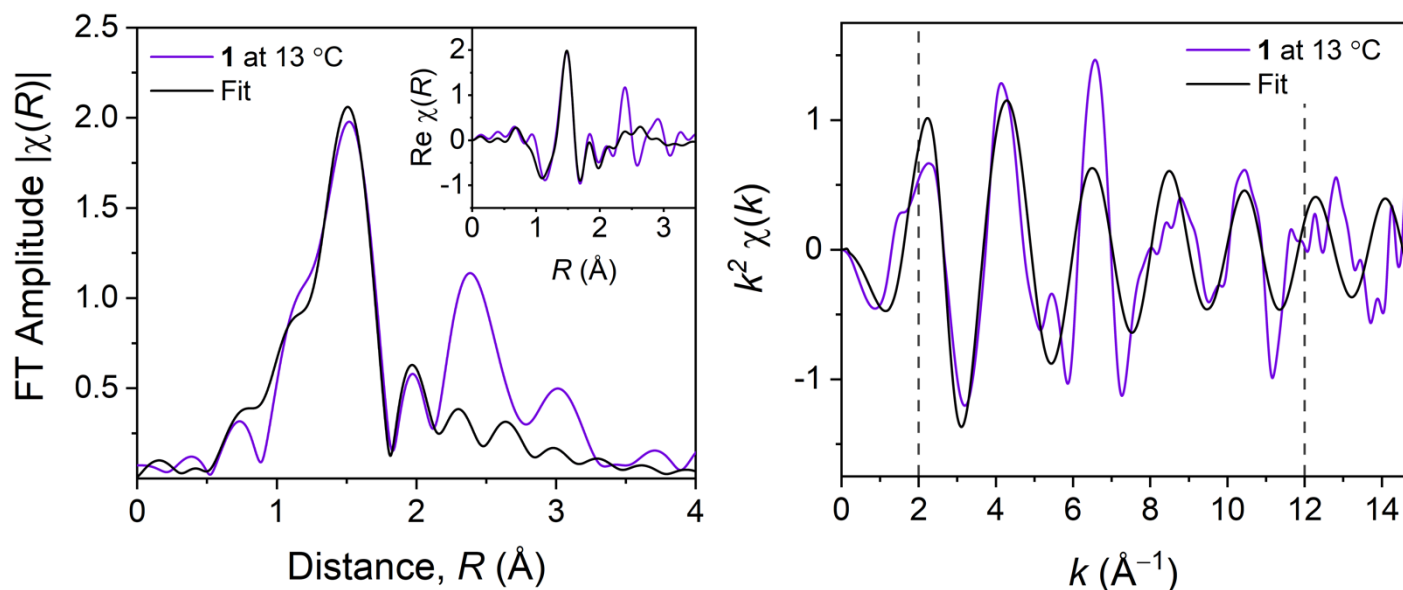


Figure S14 | Derived R -space (*left*) and k -space (*right*) plots of EXAFS fluorescence measured spectra for **1** at 13 °C at the Co K -edge ($0 - 15 \text{ \AA}^{-1}$ at $\Delta k = 0.05 \text{ \AA}^{-1}$). EXAFS data (*purple*) against simulated fits (*black*) are made with k^2 -weighting over R -range of $1.1 - 2 \text{ \AA}$ and k -range of $2 - 12 \text{ \AA}^{-1}$. **Inset:** Fit of real part of the FT EXAFS data. Fits were made according to reported crystal structure data.⁷

Table S16 | EXAFS fit parameters of single scatter pathways for **1** at 13 °C.

Path	Atom Type	N	$R_{\text{eff}} \text{ (\AA)}$	$\Delta R \text{ (\AA)}$	$r \text{ (\AA)}$	$\sigma^2 \text{ (\AA}^2\text{)}$
r_1	N	6	1.9687	-0.00991	1.95879	-0.006(1)

Common fit parameters for this set include $S_0^2 = 0.48(5)$, $E_0 = 0.1(1.1) \text{ eV}$, and $\alpha = -0.005(6)$

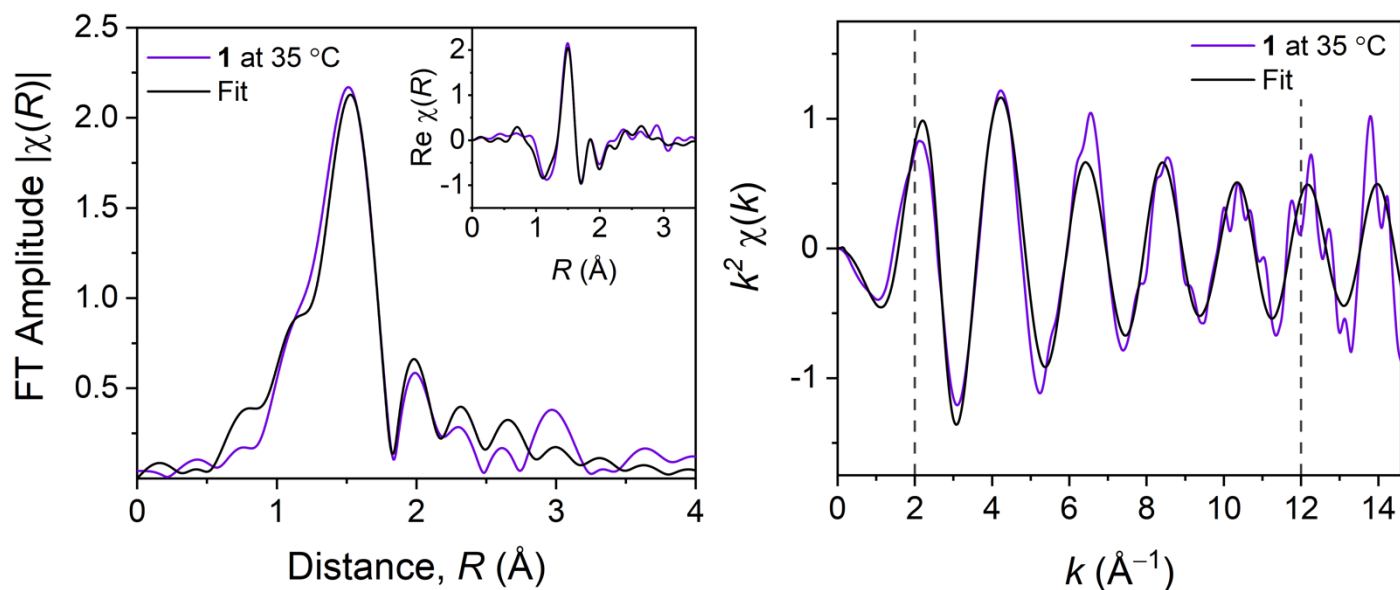


Figure S15 | Derived R -space (*left*) and k -space (*right*) plots of EXAFS fluorescence measured spectra for **1** at 35 °C at the Co K -edge (0 – 15 \AA^{-1} at $\Delta k = 0.05 \text{\AA}^{-1}$). EXAFS data (*purple*) against simulated fits (*black*) are made with k^2 -weighting over R -range of 1.1 – 2 \AA and k -range of 2 – 12 \AA^{-1} . **Inset:** Fit of real part of the FT EXAFS data. Fits were made according to reported crystal structure data.⁷

Table S17 | EXAFS fit parameters of single scatter pathways for **1** at 35 °C.

Path	Atom Type	N	R_{eff} (\AA)	ΔR (\AA)	r (\AA)	σ^2 (\AA^2)
r_1	N	6	1.9687	0.00545	1.97415	-0.001(2)

Common fit parameters for this set include $S_0^2 = 0.48(5)$, $E_0 = 0.1(1.1)$ eV, and $\alpha = 0.003(9)$

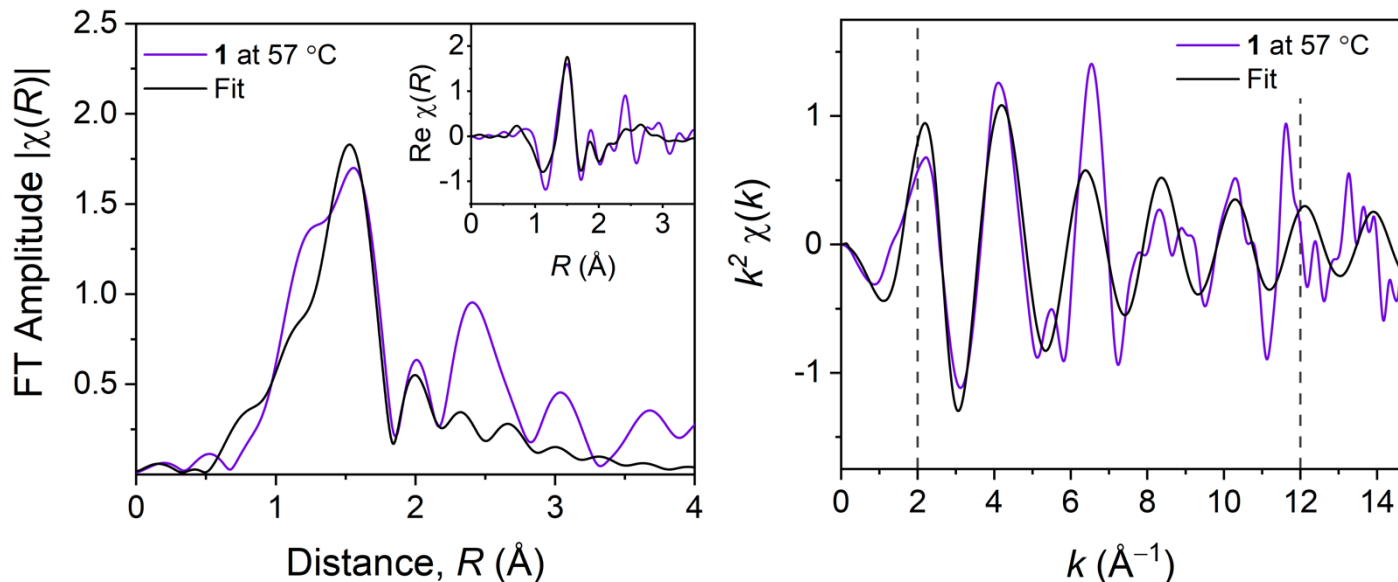


Figure S16 | Derived R -space (*left*) and k -space (*right*) plots of EXAFS fluorescence measured spectra for **1** at 57 °C at the Co K -edge ($0 - 15 \text{ \AA}^{-1}$ at $\Delta k = 0.05 \text{ \AA}^{-1}$). EXAFS data (*purple*) against simulated fits (*black*) are made with k^2 -weighting over R -range of $1.1 - 2 \text{ \AA}$ and k -range of $2 - 12 \text{ \AA}^{-1}$. **Inset:** Fit of real part of the FT EXAFS data. Fits were made according to reported crystal structure data.⁷

Table S18 | EXAFS fit parameters of single scatter pathways for **1** at 57 °C.

Path	Atom Type	N	R_{eff} (Å)	ΔR (Å)	r (Å)	σ^2 (Å ²)
r_1	N	6	1.9687	0.01488	1.98358	0.0004(16)

Common fit parameters for this set include $S_0^2 = 0.48(5)$, $E_0 = 0.1(1.1) \text{ eV}$, and $\alpha = 0.008(6)$

Table S19 | Ligand bite angles of **2** at 13 and 57 °C. Chelating N–Co–N ligand bond angle of the three separate ethylene bridging units in the temperature-specific optimized structures. The average N–Co–N bond angle of this $-0.04(1)^\circ$ from 13 to 57 °C EXAFS bond measurements.

N–Co–N Ligand Bite Angle		
13 °C	57 °C	Δ (N–Co–N)
84.938	84.919	-0.019
84.956	84.919	-0.038
84.968	84.921	-0.047

Table S20 | Ligand bite angles of **3** at 13 and 57 °C. Chelating N–Co–N ligand bond angle of the three separate trimethylene bridging units in the temperature-specific optimized structures. The average N–Co–N bond angle of this $-0.134(7)^\circ$ from 13 to 57 °C EXAFS bond measurements.

N–Co–N Ligand Bite Angle		
13 °C	57 °C	Δ (N–Co–N)
93.596	93.456	-0.140
93.565	93.428	-0.137
93.626	93.500	-0.126

Table S21 | Ligand bite angles of **5** at 13 and 57 °C. Chelating N–Co–N ligand bond angle of the three separate ethylene bridging units in the temperature-specific optimized structures. The average N–Co–N bond angle of this $-0.0830(1)^\circ$ from 13 to 57 °C EXAFS bond measurements.

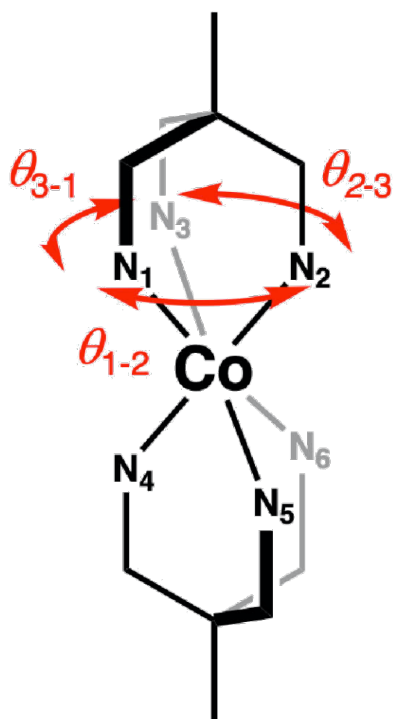
N–Co–N Ligand Bite Angle		
13 °C	57 °C	Δ (N–Co–N)
86.617	86.534	-0.083
86.618	86.535	-0.083
86.603	86.519	-0.083

Table S22 | SHAPE analysis of the change in relative geometric distortion from ideal octahedral symmetry (O_h symmetry) for optimized structures of **1-5** at 13 and 57 °C temperature-specific bond lengths. In the case of ΔS , a positive change indicates a greater distortion, while a negative change indicates an improvement of O_h symmetry. Relative changes in shape factors, $\Delta S/S(O_h)$, are made with respect to $S(O_h)$ at 13°C.

Structure	13 °C $S(O_h)$	57 °C $S(O_h)$	$\Delta S(O_h)$	$\Delta S/S(O_h)$
[Co(NH ₃) ₆]Cl ₃	0.004	0.004	0.000	0.000
[Co(en) ₃]Cl ₃	0.264	0.266	0.002	0.008
[Co(tn) ₃]Cl ₃	0.112	0.104	-0.008	-0.071
[Co(tame) ₂]Cl ₃	0.111	0.112	0.001	0.009
[Co(diNOsar)]Cl ₃	0.133	0.141	0.008	0.060

Table S23 | SHAPE analysis of the change in relative geometric distortion from ideal trigonal prismatic symmetry (D_{3h} symmetry) for optimized structures of **1-5** at 13 and 57 °C temperature-specific bond lengths. In the case of ΔS , a positive change indicates a greater distortion, while a negative change indicates an improvement of D_{3h} symmetry. Relative changes shape factors, $\Delta S/S(D_{3h})$, are made with respect to $S(D_{3h})$ at 13°C.

Structure	13 °C $S(D_{3h})$	57 °C $S(D_{3h})$	$\Delta S(D_{3h})$	$\Delta S/S(D_{3h})$
[Co(NH ₃) ₆]Cl ₃	16.627	16.627	0.000	0.000
[Co(en) ₃]Cl ₃	13.883	13.876	-0.007	-0.001
[Co(tn) ₃]Cl ₃	14.331	14.412	0.081	0.006
[Co(tame) ₂]Cl ₃	14.376	14.37	-0.006	0.000
[Co(diNOsar)]Cl ₃	14.535	14.464	-0.071	-0.005



N–Co–N Ligand Bite Angle			
	θ (13 °C)	θ (57 °C)	$\Delta\theta$
1 to 2	88.499	88.512	0.013
2 to 3	88.483	88.493	0.010
3 to 1	88.474	88.456	-0.018
4 to 5	88.473	88.460	-0.013
5 to 6	88.494	88.507	0.013
6 to 4	88.491	88.493	0.002
	Average		0.001
	Deviation		0.013615

Figure S17 | Depiction of computed changes in bite angles for the tame ligand in **4**. Note that though there are somewhat large changes to individual N–Co–N angles for the tame ligands, the average of the change is relatively minor compared with other bite angle differences (e.g. Fig 4, main text).

Table S24 | Computed coordinates of [Co(diNOsar)]³⁺ with fixed Co–N bond distances to 13 °C EXAFS (1.9701 Å, see Table S1 and S4). Total energy: –2671.56817364 Hartrees

Symbol	x	y	z
Co	-0.00001746	0.00003590	-0.00321822
N	4.58123096	-0.00315094	0.00592137
O	5.15200180	1.05047166	0.11788921
O	5.06253958	-1.10616903	-0.08148905
C	3.04267963	0.03606325	-0.00674495
C	2.61657699	-0.63751270	-1.30764245
C	2.60443849	1.49270006	0.06612590
C	2.61975460	-0.76377662	1.22397064
N	1.13429509	-0.85688789	-1.36882594
N	1.11293024	1.62559678	-0.07226585
N	1.13461047	-0.73671173	1.43054973
C	0.77482152	-2.30661580	-1.41702752
C	0.72544921	2.39301258	-1.29451749
C	0.75075595	-0.06414566	2.70851316
H	0.85892026	-0.48975260	-2.27627619
H	0.83975145	2.22096501	0.70554336
H	0.87839211	-1.71227804	1.56114915
N	-4.58129970	0.00339967	0.00593612
O	-5.15213092	-1.05040541	0.11613290
O	-5.06263912	1.10652715	-0.07958190
C	-3.04272238	-0.03590631	-0.00696511
C	-2.60458044	-1.49274200	0.06251794
C	-2.61662149	0.64062632	-1.30628830
C	-2.61973551	0.76106774	1.22562102
N	-1.11297229	-1.62537605	-0.07557432
N	-1.13426371	0.85971998	-1.36714536
N	-1.13462785	0.73356769	1.43221127
C	-0.72508818	-2.39068367	-1.29899977
C	-0.77446665	2.30939262	-1.41296566
C	-0.75087675	0.05795454	2.70858706
H	-0.84016512	-2.22202377	0.70138898
H	-0.85896733	0.49390341	-2.27515013
H	-0.87842394	1.70881076	1.56514626
H	3.13030401	-1.59491812	-1.39880718
H	2.91929234	-0.02399025	-2.15811300
H	3.09294765	2.06898438	-0.71920915
H	2.91634245	1.93259992	1.01323439
H	3.10974968	-0.35924677	2.11179481
H	2.95290640	-1.79614147	1.11652766
H	1.26969482	-2.81416218	-0.58549573

H	1.13791182	-2.76545807	-2.33857887
H	1.21719604	1.93909872	-2.15842199
H	1.07254632	3.42595367	-1.22977388
H	1.22913794	0.91780114	2.74002553
H	1.11331571	-0.62992302	3.56885253
H	-3.09274116	-2.06709921	-0.72446352
H	-2.91685934	-1.93496575	1.00839086
H	-3.13006543	1.59839745	-1.39512349
H	-2.91961483	0.02924136	-2.15821322
H	-3.10975741	0.35444850	2.11246531
H	-2.95290167	1.79369268	1.12056144
H	-1.21671961	-1.93533345	-2.16222529
H	-1.07207745	-3.42377800	-1.23611031
H	-1.26934184	2.81569904	-0.58068310
H	-1.13730146	2.76983871	-2.33382016
H	-1.22925360	-0.92407893	2.73766406
H	-1.11355041	0.62164207	3.57024759

Table S25 | Computed coordinates of [Co(diNOsar)]³⁺ with fixed Co–N bond distances to 57 °C EXAFS (1.9776 Å, see Table S1 and S6). Total energy: –2671.56901712 Hartrees

Symbol	x	y	z
Co	-0.00000394	0.00001705	-0.00309016
N	4.58310477	-0.00331242	0.00579444
O	5.15430137	1.05067177	0.11198244
O	5.06432835	-1.10676566	-0.07619557
C	3.04396908	0.03612525	-0.00686273
C	2.61992135	-0.64370393	-1.30580020
C	2.60781655	1.49426353	0.05932452
C	2.62305883	-0.75871051	1.22847312
N	1.13826676	-0.86234475	-1.37196989
N	1.11684222	1.63114810	-0.07537517
N	1.13863874	-0.73653537	1.43709837
C	0.77520724	-2.31099708	-1.41621649
C	0.72547541	2.39479222	-1.29840122
C	0.75107731	-0.06112315	2.71212084
H	0.86377912	-0.49516418	-2.27963162
H	0.84488031	2.22650152	0.70282627
H	0.88351074	-1.71231837	1.56790199
N	-4.58312654	0.00343664	0.00578447
O	-5.15435512	-1.05062900	0.11105055
O	-5.06432262	1.10695801	-0.07523002
C	-3.04398265	-0.03605229	-0.00692913
C	-2.60788098	-1.49427581	0.05758643

C	-2.61993333	0.64521743	-1.30511220
C	-2.62303782	0.75739030	1.22929026
N	-1.11685815	-1.63103358	-0.07705181
N	-1.13825964	0.86379692	-1.37108781
N	-1.13864254	0.73491282	1.43794780
C	-0.72534955	-2.39354495	-1.30072148
C	-0.77507403	2.31243438	-1.41405256
C	-0.75116900	0.05789192	2.71213940
H	-0.84503040	-2.22708013	0.70067201
H	-0.86377266	0.49733522	-2.27903973
H	-0.88347660	1.71051492	1.57000202
H	3.13321887	-1.60194808	-1.39064537
H	2.92632418	-0.03461202	-2.15817102
H	3.09560995	2.06519062	-0.73040385
H	2.92369718	1.93843926	1.00310301
H	3.11263791	-0.34803645	2.11374525
H	2.95984531	-1.79040456	1.12580813
H	1.26788604	-2.81698887	-0.58240125
H	1.13876502	-2.77354322	-2.33578711
H	1.21496063	1.93824021	-2.16224427
H	1.07293667	3.42791063	-1.23774188
H	1.22716982	0.92203199	2.74115790
H	1.11408902	-0.62327913	3.57470235
H	-3.09554043	-2.06425119	-0.73291341
H	-2.92390153	-1.93958212	1.00077382
H	-3.13314407	1.60360959	-1.38883629
H	-2.92642109	0.03712980	-2.15817380
H	-3.11267998	0.34576658	2.11408182
H	-2.95977599	1.78921810	1.12775094
H	-1.21480643	-1.93620722	-2.16417054
H	-1.07277590	-3.42673410	-1.24104698
H	-1.26774970	2.81773726	-0.57982283
H	-1.13857477	2.77581824	-2.33322696
H	-1.22725878	-0.92530459	2.73988872
H	-1.11426180	0.61894648	3.57540362

Table S26 | Computed coordinates of $[\text{Co}(\text{tame})_2]^{3+}$ with fixed Co–N bond distances to 13 °C EXAFS (1.9700 Å, see Table S1 and S7). Total energy: –2109.54797542 Hartrees

Symbol	x	y	z
Co	-0.00000347	0.00026855	0.00013800
N	-1.16688756	-1.36565803	0.80857250
N	-1.16696618	-0.01657170	-1.58695199
N	1.16676891	-1.43273672	-0.68256134

N	-1.16734922	1.38306928	0.77866627
N	1.16708267	1.30778504	-0.89944564
N	1.16729811	0.12585389	1.58209106
C	-4.64680352	-0.00048948	-0.00030824
C	-3.11426948	-0.00032950	-0.00007533
C	-2.60840971	-0.99667970	1.04747613
C	-2.60810793	-0.40917475	-1.38666869
C	-2.60868229	1.40509670	0.33918814
C	2.60826729	-1.08671343	-0.95383579
C	3.11426447	-0.00023486	-0.00017904
C	4.64681594	-0.00052409	-0.00019484
C	2.60847624	-0.28292936	1.41761373
C	2.60857697	1.36906715	-0.46396050
H	-1.17927408	-2.17178325	0.18471381
H	-0.80696977	-0.57782351	-2.35828537
H	0.80665405	-1.89602002	-1.51638867
H	-1.17997696	1.24590158	1.78872434
H	1.17923630	1.08134022	-1.89329024
H	0.80760127	-0.36408281	2.40072487
H	-5.03823579	-0.94835206	-0.37485339
H	-5.03853196	0.14911460	1.00771240
H	5.03838498	0.05747337	-1.01767911
H	-3.20353192	-1.91097901	1.02017900
H	-2.69895608	-1.48658235	-1.53877537
H	-2.70038243	2.07558247	-0.51769056
H	3.20329668	-1.99490842	-0.84440876
H	2.69952799	-1.34231745	1.66583596
H	3.20387882	1.72857178	-1.30491224
H	-0.80689062	-1.75209423	1.68070945
H	-1.17997355	0.92696462	-1.97264836
H	1.17920999	-2.17956753	0.01117579
H	-0.80782756	2.33182585	0.67758156
H	0.80731307	2.26165035	-0.88315728
H	1.18025773	1.10015339	1.88164753
H	-5.03831812	0.79772414	-0.63398939
H	5.03817798	-0.91082842	0.45821381
H	5.03854261	0.85151785	0.55884749
H	-2.70025774	-0.59009094	2.05666919
H	-3.20369694	0.07083907	-2.16494168
H	-3.20413793	1.83859331	1.14439121
H	2.70008237	-0.77266469	-1.99553305
H	3.20416550	0.26513040	2.14947802
H	2.70033074	2.11373663	0.32929369

Table S27 | Computed coordinates of $[\text{Co}(\text{tame})_2]^{3+}$ with fixed Co–N bond distances to 57 °C EXAFS (1.9707 Å, see Table S1 and S9). Total energy: –2109.54796698 Hartrees

Symbol	x	y	z
Co	-0.00002601	0.00074305	0.00055857
N	-1.16688893	-1.54889778	0.34769887
N	-1.16733941	0.47520857	-1.51460612
N	1.16675876	-1.15213634	-1.09166143
N	-1.16810024	1.07590680	1.16807191
N	1.16767954	1.52238978	-0.45167702
N	1.16772835	-0.36794571	1.54454054
C	-4.64682460	-0.00154565	-0.00119689
C	-3.11412683	-0.00082791	-0.00051572
C	-2.60842817	-1.27169381	0.68852041
C	-2.60803758	0.03871999	-1.44557743
C	-2.60969110	1.23131967	0.75641952
C	2.60821662	-0.73969065	-1.24293472
C	3.11427754	-0.00076721	-0.00048792
C	4.64695022	-0.00148864	-0.00069595
C	2.60846886	-0.70707874	1.26107404
C	2.60951949	1.44510545	-0.01941544
H	-1.17864676	-2.12277741	-0.49468067
H	-0.80677893	0.18135110	-2.42188505
H	0.80647093	-1.33571692	-2.02762587
H	-1.18032488	0.63333990	2.08627004
H	1.17922811	1.61357971	-1.46689901
H	0.80765614	-1.08528670	2.17329448
H	-5.03765208	-0.78714590	-0.65084548
H	-5.03866420	-0.17150296	1.00355136
H	5.03852600	0.36689361	-0.95091189
H	-3.20353399	-2.13294357	0.38048083
H	-2.69793646	-0.93916962	-1.92286281
H	-2.70185214	2.13368231	0.14862430
H	3.20324055	-1.63726316	-1.41932402
H	2.69853199	-1.79138387	1.16989326
H	3.20474362	2.04584415	-0.70905859
H	-0.80705120	-2.18569275	1.05802044
H	-1.18119961	1.49184356	-1.58780778
H	1.17882710	-2.07632818	-0.66170068
H	-0.80936177	2.00981834	1.36466970
H	0.80878644	2.42471475	-0.14101085
H	1.18162678	0.46749007	2.12848500
H	-5.03858883	0.95345192	-0.35680223

H	5.03791828	-1.00886567	0.15516446
H	5.03882367	0.63688084	0.79356489
H	-2.70034793	-1.19588617	1.77386806
H	-3.20431575	0.73503032	-2.03755347
H	-3.20537625	1.39429482	1.65606938
H	2.69999732	-0.11896823	-2.13648700
H	3.20491356	-0.41235309	2.12607724
H	2.70222954	1.90901407	0.96463377

Table S28 | Computed coordinates of $[\text{Co}(\text{tn})_3]^{3+}$ with fixed Co–N bond distances to 13 °C EXAFS (1.9825 Å, see Table S1 and S10). Total energy: –2071.43715806 Hartrees

Symbol	x	y	z
Co	0.00082394	-0.00002603	-0.09780114
C	-1.67282784	-2.17837128	1.24936642
C	-1.77491496	-2.90315556	-0.07575167
C	-0.45650228	-2.95717548	-0.81567793
C	2.72373640	-0.35588755	1.25023271
C	3.40342413	-0.08269594	-0.07456158
C	2.78952128	1.08354880	-0.81730302
C	-1.05366242	2.53618474	1.24881154
C	-1.63271379	2.98669205	-0.07539859
C	-2.33446143	1.87051619	-0.81725600
H	-2.32720288	-0.32451903	0.73126376
H	0.41907415	1.33548225	1.99310469
H	-1.98804116	0.03629590	-1.61380668
H	-0.95854105	1.14261209	-2.12762713
H	-0.85379547	-2.58105273	1.84953281
H	-2.58662465	-2.30451453	1.83258381
H	-2.09174256	-3.92988912	0.11991995
H	-2.56551387	-2.47155450	-0.70155007
H	0.31912715	-3.38878179	-0.17824541
H	-0.52689688	-3.59751468	-1.69644582
H	2.66029410	0.55557102	1.84890315
H	-1.35844103	-0.30601111	1.99696177
H	3.29070317	-1.08209232	1.83525507
H	4.45033630	0.15869951	0.12176674
H	3.42733950	-0.98422107	-0.69877502
H	2.77380214	1.97243504	-0.18182372
H	3.37933387	1.34169038	-1.69833838
H	-1.80950426	2.02467818	1.84901788
H	-0.70867367	3.39119469	1.83278618
H	-2.36652370	3.77124442	0.12169140
H	-0.86559572	3.45953241	-0.70061152

H	-3.09585915	1.41190671	-0.18150223
H	0.96371313	-1.74425618	-1.61006990
H	-2.85369763	2.25109730	-1.69833702
H	-0.50697896	-1.40254490	-2.12753042
H	1.44978775	-1.85200810	0.72960481
H	0.94638533	-1.02549379	1.99625442
H	1.02889230	1.70249829	-1.61480012
H	1.47028817	0.25694854	-2.12763835
H	0.87830325	2.18373158	0.72399074
N	-1.44260765	-0.70684239	1.06281267
N	0.01216135	-1.59799250	-1.27103737
N	1.33570777	-0.89553023	1.06248588
N	1.37871252	0.80669814	-1.27284486
N	0.10896238	1.60574993	1.05973859
N	-1.38802044	0.78814600	-1.27253716

Table S29 | Computed coordinates of $[\text{Co}(\text{tn})_3]^{3+}$ with fixed Co–N bond distances to 57 °C EXAFS (1.9910 Å, see Table S1 and S12). Total energy: -2071.43833732 Hartrees

Symbol	x	y	z
Co	-0.00091913	0.00005460	-0.09993031
C	1.72968398	2.13716024	1.25236300
C	1.85144179	2.86009847	-0.07230998
C	0.53644922	2.94992895	-0.81524822
C	-2.71742800	0.42655991	1.25256303
C	-3.40500936	0.16936571	-0.07155763
C	-2.82267295	-1.01201418	-0.81618102
C	0.98951459	-2.56553382	1.25119378
C	1.55848757	-3.03101633	-0.07235868
C	2.28925096	-1.93460636	-0.81601186
H	2.34132165	0.26906883	0.73050887
H	-0.45779294	-1.33147320	1.99363145
H	1.98946628	-0.09600752	-1.62353816
H	0.93088217	-1.17886382	-2.13045624
H	0.91876822	2.55806185	1.85103449
H	2.64498254	2.24285247	1.83737078
H	2.19439061	3.87812225	0.12486583
H	2.63166053	2.40889669	-0.69730107
H	-0.22950832	3.39928041	-0.17841510
H	0.62603808	3.59136791	-1.69351736
H	-2.67443393	-0.48607554	1.85122464
H	1.37320310	0.27046558	1.99824246
H	-3.26757078	1.16536513	1.83795045
H	-4.45726013	-0.04589608	0.12672119

H	-3.40781805	1.07112552	-0.69585205
H	-2.82586075	-1.90074000	-0.18032877
H	-3.42307162	-1.25584902	-1.69418928
H	1.75661485	-2.07054049	1.85094231
H	0.62567150	-3.41220418	1.83595691
H	2.27228444	-3.83342082	0.12643404
H	0.78040694	-3.48546184	-0.69764691
H	3.05985762	-1.49237972	-0.17978890
H	-0.91269171	1.77637865	-1.61836573
H	2.80144699	-2.33157641	-1.69402653
H	0.55100365	1.39630437	-2.13101869
H	-1.40888765	1.89244371	0.72838000
H	-0.92373748	1.05619792	1.99704980
H	-1.08177060	-1.67342844	-1.62486358
H	-1.48821784	-0.21430680	-2.13037627
H	-0.93346219	-2.16888362	0.72203913
N	1.46708930	0.67173276	1.06530006
N	0.03373440	1.60560892	-1.27677211
N	-1.31810450	0.93461726	1.06436240
N	-1.40824592	-0.77055848	-1.27872162
N	-0.15177676	-1.61004144	1.06144599
N	1.37167413	-0.83135239	-1.27836670

Table S30 | Computed coordinates of $[\text{Co}(\text{en})_3]^{3+}$ with fixed Co–N bond distances to 13 °C EXAFS (1.9694 Å, see Table S1 and S13). Total energy: –1953.43347520 Hartrees

Symbol	x	y	z
Co	0.00007964	-0.00016764	0.00031164
C	0.89173474	2.61316490	0.74934824
C	1.93710856	-1.96657225	-0.75055951
C	1.81808218	-2.07805438	0.74955723
H	2.33267589	0.03607462	-1.00890472
H	1.34069901	-0.54747408	-2.11808332
H	-0.20836619	-2.32363484	1.00909271
H	0.44794361	-1.37804768	2.11816861
H	-0.01304352	2.95425925	1.25776881
H	1.71480354	3.23941669	1.09739793
H	1.26909287	-2.66591634	-1.25866368
H	2.94996663	-2.17393474	-1.09966290
H	1.94948155	-3.10385570	1.09776376
H	2.56565918	-1.46460195	1.25776887
H	0.96971114	1.07658492	2.11793816
H	2.11693722	0.98039701	1.00921898
N	1.12140551	1.17432481	1.11460698

N	1.51985922	-0.57045710	-1.11481094
N	0.45704447	-1.55820877	1.11482917
N	-0.26612128	1.60160367	-1.11410483
N	-1.57760981	0.38357793	1.11480421
N	-1.25450187	-1.03166537	-1.11346394
C	0.73478814	2.66094359	-0.75065921
H	-0.19787894	1.43513017	-2.11752539
H	-1.19758324	2.00245317	-1.00684595
C	-2.70964608	-0.53377578	0.74943529
H	-1.90632569	1.34313450	1.00988501
H	-1.41701885	0.30042019	2.11807296
C	-2.67226774	-0.69412936	-0.75040950
H	-1.13604536	-2.03871317	-1.00570662
H	-1.14472574	-0.88993256	-2.11700203
H	1.67416681	2.43263471	-1.25948063
H	0.40747357	3.64181683	-1.09929780
H	-2.55401465	-1.48777875	1.25846218
H	-3.66332902	-0.13301734	1.09679191
H	-3.35815306	-1.46795921	-1.09904477
H	-2.94360960	0.23338406	-1.25982596

Table S31 | Computed coordinates of $[\text{Co}(\text{en})_3]^{3+}$ with fixed Co–N bond distances to 57 °C EXAFS (1.9714 Å, see Table S1 and S15). Total energy: –1953.43280799 Hartrees

Symbol	x	y	z
Co	0.00019508	0.00004906	0.00060861
C	2.75615827	0.19294588	0.74938480
C	-1.06182947	-2.54904138	-0.75088589
C	-1.21193373	-2.48274823	0.74925518
H	0.93861878	-2.13851295	-1.00506315
H	0.01928172	-1.45134510	-2.11780278
H	-2.22332871	-0.70966434	1.00992409
H	-1.09728881	-0.94900061	2.11899024
H	2.71984672	1.15957439	1.25716555
H	3.65296814	-0.32234108	1.09726475
H	-1.96485164	-2.20381558	-1.25968768
H	-0.86092912	-3.56328343	-1.09985472
H	-2.10707252	-3.00122634	1.09666328
H	-0.35720846	-2.93496034	1.25762390
H	1.37091940	-0.47430937	2.11939392
H	1.72702692	-1.56974655	1.01095750
N	1.51975921	-0.57689452	1.11613569
N	0.06469696	-1.62455438	-1.11422003

N	-1.26005644	-1.02695564	1.11567238
N	1.37489372	0.86744891	-1.11481097
N	-0.25994628	1.60522255	1.11509697
N	-1.43824840	0.75621346	-1.11538221
C	2.73877837	0.35477460	-0.75085231
H	1.24780399	0.74021766	-2.11825263
H	1.38301300	1.88137356	-1.00699630
C	-1.54567948	2.28972792	0.74914383
H	0.49539222	2.28187817	1.00844047
H	-0.27296466	1.42592823	2.11854793
C	-1.67751974	2.19355820	-0.75105813
H	-2.32006227	0.25548143	-1.00845364
H	-1.26365264	0.71020521	-2.11868480
H	2.89146450	-0.60028826	-1.25885022
H	3.51666532	1.03568240	-1.10024273
H	-2.36384022	1.77411307	1.25732587
H	-1.54868110	3.32398979	1.09715355
H	-2.65649283	2.52592546	-1.10025295
H	-0.92743153	2.80413543	-1.25910970

Table S32 | Computed coordinates of $[\text{Co}(\text{NH}_3)_6]^{3+}$ with fixed Co–N bond distances to 13 °C EXAFS (1.9588 Å, see Table S1 and S16). Total energy: –1721.20216299 Hartrees

Symbol	x	y	z
Co	-0.00001889	-0.00000617	0.00000120
N	1.23807732	-0.97098441	1.16669648
H	1.78259482	-0.38630969	1.80596446
H	1.95122903	-1.51101564	0.66940526
H	0.80542103	-1.66177330	1.78498900
N	0.48552315	1.68448014	0.87385107
H	-0.13871341	2.47064657	0.67567895
H	1.41090659	2.04586543	0.62854990
H	0.50636052	1.64558130	1.89636500
N	1.45610061	0.26386165	-1.28333376
H	1.40732521	1.13128276	-1.82367941
H	1.54365264	-0.46044526	-2.00069314
H	2.38872844	0.29887086	-0.86326792
N	-1.45607156	-0.26407391	1.28337085
H	-1.54303461	0.45957597	2.00146542
H	-1.40769501	-1.13206783	1.82283516
H	-2.38881729	-0.29815387	0.86349021
N	-0.48575199	-1.68446668	-0.87379222
H	-1.41128750	-2.04555103	-0.62862450
H	0.13820269	-2.47080410	-0.67541439

H	-0.50639798	-1.64569411	-1.89631437
N	-1.23784637	0.97119472	-1.16679388
H	-1.95280266	1.50897871	-0.66965982
H	-1.78018484	0.38702110	-1.80836607
H	-0.80519576	1.66407819	-1.78274598

Table S33 | Computed coordinates of $[\text{Co}(\text{NH}_3)_6]^{3+}$ with fixed Co–N bond distances to 57 °C EXAFS (1.9836 Å, see Table S1 and S18). Total energy: –1721.20581740 Hartrees

Symbol	x	y	z
Co	-0.00001858	-0.00000606	0.00000108
N	1.25528531	-0.98001056	1.18253798
H	1.79618280	-0.39028822	1.81965342
H	1.96775020	-1.51763193	0.68243655
H	0.81976929	-1.66965194	1.79950325
N	0.48825966	1.70738106	0.88374524
H	-0.13978910	2.48919903	0.68231310
H	1.41321450	2.06683318	0.63553956
H	0.50797699	1.66530460	1.90578106
N	1.47425987	0.26890645	-1.29952933
H	1.42010076	1.13652956	-1.83834885
H	1.55941632	-0.45768724	-2.01434132
H	2.40475989	0.30520960	-0.87578829
N	-1.47422984	-0.26911947	1.29956613
H	-1.55879797	0.45682296	2.01511003
H	-1.42046935	-1.13731304	1.83750919
H	-2.40484908	-0.30449342	0.87600825
N	-0.48849026	-1.70736782	-0.88368519
H	-1.41360399	-2.06650961	-0.63562506
H	0.13926809	-2.48936149	-0.68203356
H	-0.50799950	-1.66542261	-1.90572992
N	-1.25505345	0.98022185	-1.18263617
H	-1.96931892	1.51559278	-0.68269019
H	-1.79377643	0.39099630	-1.82204745
H	-0.81955193	1.67195456	-1.79726960

References

1. R. A. Krause, E. A. Megargle, *J. Chem. Educ.*, **1976**, *53*, 6268.
2. J. C. Bailar Jr., J. B. Work, *J. Am. Chem. Soc.*, **1946**, *68*, 232.
3. R. J. Geue, M. R. Snow, *Inorg. Chem.*, **1977**, *16*, 231.
4. C.-J. Qin, L. James, J. D. Chartres, L. J. Alcock, K. J. Davis, A. C. Willis, A. M. Sargeson, P. V. Bernhardt, S. F. Ralph, *Inorg. Chem.*, **2011**, *50*, 9131.
5. G. A. Bottomley, I. J. Clark, I. I. Creaser, L. M. Engelhardt, R. J. Geue, K. S. Hagen, J. M. Harrowfield, G. A. Lawrance, P. A. Lay, A. M. Sargeson, A. J. See, B. W. Skelton, A. H. White, F. R. Wilner, *Aust. J. Chem.*, **1994**, *47*, 143.
6. B. Ravel, M. Newville, *J. Synchrotron Radiat.*, **2005**, *12*, 537.
7. G. J. Kruger, E. C. Reynhardt, *Acta Crystallogr., Sect. B: Struct. Sci, Cryst. Eng. Mater.*, **1978**, *B34*, 915.
8. K. Nakatsu, Y. Saito, H. Kuroya, *Bull. Chem. Soc. Jpn.*, **1956**, *29*, 428.
9. R. Nagao, F. Marumo, Y. Saito, *Acta Crystallogr., Sect. B: Struct. Sci, Cryst. Eng. Mater.*, **1973**, *B29*, 2438.
10. R. J. Geue, M. R. Snow, *Inorg. Chem.*, **1977**, *16*, 231.
11. I. J. Clark, R. J. Geue, L. M. Engelhardt, J. M. Harrowfield, A. M. Sargeson, W. H. White, *Aust. J. Chem.*, **1993**, *46*, 1485.
12. B. Ravel, *J. Synchrotron Radiat.*, **2001**, *8*, 314-316.
13. Bencini, A.; Bianchi, A.; Garcia-España, E.; Micheloni, M.; Ramirez, J. A.; *Coord. Chem. Rev.*, **1999**, *188*, 97.
14. Mizuno, Y.; Yokote, A.; Iida, M. *Bull. Chem. Soc. Jpn.*, **1997**, *70*, 2437.
15. Seward, T. M.; Henderson, C. M. B.; Charnock, J. M.; Dobson, B. R. *Geochim. Cosmochim. Acta*, **1996**, *60*, 13, 2273–2282.
16. Sharma, M.; Tripathi, J.; Mishra, A.; Yadav, A. K.; Jha, S. N.; Shrivastava, B. D. *Mater. Today: Proc.*, **2019**, *12*, 614-620.
17. J. Purans, J. Timoshenko, A. Kuzmin, G. Dalba, P. Fornasini, R. Grisenti, N. D. Afify, F. Rocca, S. De Panfilis, I. Ozhogin, *J. Phys. Conf. Ser.*, **2009**, *190*, 012063.
18. J. Purans, N. D. Afify, G. Dalba, R. Grisenti, S. De Panfilis, A. Kuzmin, V. I. Ozhogin, F. Rocca, A. Sanson, S. I. Tiutiunnikov, P. Fornasini, *Phys. Rev. Lett.*, **2008**, *100*, 055901.
19. J. Purans, G. Dalba, P. Fornasini, A. Kuzmin, S. De Panfilis, F. Rocca, *AIP Conference Proceedings*; AIP: Stanford, California (USA), **2007**; Vol. 882, pp 422–424.
20. G. Dalba, P. Fornasini, R. Grisenti, J. Purans, *Phys. Rev. Lett.*, **1999**, *82*, 4240.
21. N. Adb el All, G. Dalba, D. Diop, P. Fornasini, R. Grisenti, O. Mathon, F. Rocca, B. Thiodjio Sendja, M. Vaccari, *J. Phys.: Condens. Matter*, **2012**, *24*, 115403.
22. M. J. Frisch, G. W. Trucks, H. B. Schlegel, G. E. Scuseria, M. A. Robb, J. R. Cheeseman, G. Scalmani, V. Barone, G. A. Petersson, H. Nakatsuji, X. Li, M. Caricato, A. V. Marenich, J. Bloino, B. G. Janesko, R. Gomperts, B. Mennucci, H. P. Hratchian, J. V. Ortiz, A. F. Izmaylov, J. L. Sonnenberg, D. Williams-Young, F. Ding, F. Lipparini, F. Egidi, J. Goings, B. Peng, A. Petrone, T. Henderson, D. Ranasinghe, V. G. Zakrzewski, J. Gao, N. Rega, G. Zheng, W. Liang, M. Hada, M. Ehara, K. Toyota, R. Fukuda, J. Hasegawa, M. Ishida, T. Nakajima, Y. Honda, O. Kitao, H. Nakai, T. Vreven, K. Throssell, J. A. Jr. Montgomery, J. E. Peralta, F. Ogliaro, M. J. Bearpark, J. J. Heyd, E. N. Brothers, K. N. Kudin, V. N.

Staroverov, T. A. Keith, R. Kobayashi, J. Normand, K. Raghavachari, A. P. Rendell, J. C. Burant, S. S. Iyengar, J. Tomasi, M. Cossi, J. M. Millam, M. Klene, C. Adamo, R. Cammi, J. W. Ochterski, R. L. Martin, K. Morokuma, O. Farkas, J. B. Foresman, D. J. Fox, Gaussian 16, Revision A.03; Gaussian, Inc.: Wallingford, CT, 2016.

23. F. Neese, *J. Chem. Phys.*, **2003**, 119, 9428–9443.

24. R. Krishnan, J. S. Binkley, R. Seeger, J. A. Pople, *J. Chem. Phys.*, **1980**, 72, 650–654.

25. S. Alvarez, D. Avnir, M. Llunell, M. Pinsky, *New J. Chem.*, **2002**, 26, 996.

26. S. Alvarez, P. Alemany, D. Casanova, J. Cirera, M. Llunell, D. Avnir, *Coord. Chem. Rev.*, **2005**, 249, 1693.

27. M. Pinsky, D. Avnir, *Inorg. Chem.*, **1998**, 37, 5575.